

## BEST AVAILABLE COPY

AMENDMENT UNDER 37 C.F.R. § 1.116  
U.S. Application No.: 10/656,124

Attorney Docket Q76661

### **REMARKS**

In the present Amendment, the specification has been amended for clarity.

Claim 1 has been amended to improve its form and/or for clarity. These amendments are not to be deemed to narrow the scope of the claim.

Claim 7 has been amended to be consistent with claim 1 as amended.

Claims 22 and 23 have been added. Claim 22 is supported by the specification, for example, original claims 1, 6 and 7. Claim 23 is supported by the specification, for example, original claims 1, 8, 9 and 13.

No new matter has been added and entry of the Amendment is respectfully requested. Upon entry of the Amendment, claims 1-23 will be all the claims pending in the application.

Applicants note with appreciation that all of the previous prior art rejections have been withdrawn. See Paragraph No. 5 of the Office Action.

#### **I. Response to Claim Objection**

Claims 1-15 are objected to for informalities.

Applicants respectfully submit that the present claims do not have informalities.

Applicants have in the Amendment, amended claim 1 to add “the” before “surface projections” in step (d). Accordingly, the Examiner is respectfully requested to reconsider and withdraw the objection.

**II. Response to Rejection Under 35 U.S.C. § 112, First Paragraph**

Claims 1-15 are rejected under 35 U.S.C. § 112, first paragraph, as allegedly failing to comply with the written description requirement.

Applicants respectfully traverse the rejection. Step (c) recited in present claim 1 is substantially the same as that in original claim 1. In addition, claim 7 is substantially the same as original claim 7. The amendments to claims 1 (in particular, step (c)) and 7 are merely for formal matters, i.e., to improve their form and/or for clarity. According to MPEP 608.01(I), original claims are part of the original disclosure of an application. Accordingly, the subject matter of step (c) of present claim 1 as well as claim 7 are not new matter.

In addition, Applicants have in the Amendment, amended claim 1, step (c), to recite control of state of polymerization based on variation of the index of refraction of the layer.

Further, the concept underlying step (c) of present claim 1 is that the state of polymerization of the layer is controlled (i.e., monitored) by detecting variations in the index of refraction thereof. The present specification describes at page 2, lines 18-19, that the layer is exposed to UV radiation and the state of polymerization thereof is controlled. The same concept is repeated at page 5, lines 17-18 of the present specification. Further, at page 6, line 11 of the present specification, a description is provided for a system used for monitoring the state of polymerization, which includes laser 19 and camera 20.

The state of polymerization is monitored by detecting the index of refraction of the layer, and consequently changing the intensity of the applied magnetic or electrical field (see also original claim 7). The above detection is performed in an indirect manner, i.e., by detecting the

distribution of the intensities of the orders of diffraction in areas of the layer having different degrees of cross-linking, which distribution indeed results in different indexes of refraction, as noted by the Examiner.

In view of the foregoing, Applicants respectfully submit that the subject matter contained in step (c) of present claim 1 as well as claim 7 are sufficiently described in the specification as originally filed, and thus the rejection should be withdrawn.

**III. Response to Rejection Under 35 U.S.C. § 112, Second Paragraph**

Claims 1-15 are rejected under 35 U.S.C. § 112, second paragraph, as allegedly being indefinite.

In the Amendment filed November 28, 2005, Applicants explained that the terms “binary mask,” “half-tone mask,” “nanoparticle” and “ferrofluids” contained in the present claims are well-known in the art and the meanings thereof are understood.

For the Examiner’s consideration, Applicants submit herewith a copy of the following mentioned documents, except for the U.S. patents, and the following additional explanation.

Nanoparticles: A “nanoparticle” is a microscopic particle whose size is measured in nanometers, wherein the nanometer scale generally means a diameter up to 100 nm. See “*Handbook of Nanostructured Materials and Nanotechnology*”, published in 2000 (see copyright clause at page 2). The “Foreword” of the book identifies what is generally meant by nanometric scale (i.e., 1-100 nanometers).

Ferrofluids: “Ferrofluids” are mentioned in, for example, USP 6,180,226 to McArdle et al cited by the Examiner in the Office Action mailed July 28, 2005 (see, e.g., “Abstract” and “Description of Related Technology” thereof). In addition, “*Magnetoviscous Effects in Ferrofluids*”, published in 2002, describes that ferrofluids have been known since the beginning of 1960s (see Preface, Sections 1.1 and 1.3).

Halftone mask: The term “halftone mask” is mentioned, for example, in USP 5,744,381 and USP 5,723,236; “*Multilevel Diffractive Optical Element Manufacture by Excimer Laser Ablation and Halftone Masks*” by Holmes et al, Proc. Of LASE 2001, San Jose, CA, January 19-26, 2001; and “*Microstructuring by Excimer Laser*” by Harvey, SPIE, vol. 2639, October 23, 1995.

Binary mask: The term “binary mask” is mentioned, for example, in USP 5,326,659 and USP 5,888,678; “*Multilevel Diffractive Optical Element Manufacture by Excimer Laser Ablation and Halftone Masks*” by Holmes et al, Proc. Of LASE 2001, San Jose, CA, January 19-26, 2001; and “*Microstructuring by Excimer Laser*” by Harvey, SPIE, vol. 2639, October 23, 1995.

In view of the above, the Examiner is respectfully requested to reconsider and withdraw the rejection.

#### **IV. Conclusion**

In view of the above, reconsideration and allowance of this application are now believed to be in order, and such actions are hereby solicited. If any points remain in issue which the

AMENDMENT UNDER 37 C.F.R. § 1.116  
U.S. Application No.: 10/656,124

Attorney Docket Q76661

Examiner feels may be best resolved through a personal or telephone interview, the Examiner is kindly requested to contact the undersigned at the telephone number listed below.

The USPTO is directed and authorized to charge all required fees, except for the Issue Fee and the Publication Fee, to Deposit Account No. 19-4880. Please also credit any overpayments to said Deposit Account.

Respectfully submitted,



---

Fang Liu  
Registration No. 51,283

SUGHRUE MION, PLLC  
Telephone: (202) 293-7060  
Facsimile: (202) 293-7860

WASHINGTON OFFICE

**23373**

CUSTOMER NUMBER

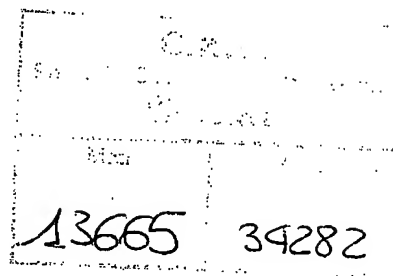
Date: June 22, 2006

# Handbook of Nanostructured Materials and Nanotechnology

Volume 1  
Synthesis and Processing

Edited by

Harl Singh Nalwa, M.Sc., Ph.D.  
Hitachi Research Laboratory  
Hitachi Ltd., Ibaraki, Japan



1



**ACADEMIC PRESS**

A Harcourt Science and Technology Company

San Diego San Francisco New York Boston  
London Sydney Tokyo

The images for the cover of this book were reprinted with generous permission from:

(Top left) R.P. Andres, J.D. Bielefeld, J.I. Henderson, D.B. Janes, V.R. Kolagunta, C.P. Kubiak, W. Mahoney, and R.G. Osifchin, *Science* 273, 1690 (1996). Copyright 1996 American Association for the Advancement of Science.

(Top right) Bruce Godfrey, Volume 5, Chapter 12 in this series.

(Middle left) M.R. Sorensen, K.W. Jacobsen, and P. Stoltze, *Phys. Rev. B* 53, 2101-2113, © 1996 American Physical Society.

(Middle right) T.W. Ebbesen et al., *Nature* 382, 54 (1996) copyright 1996 Macmillan Magazines Ltd.

(Bottom left) R.H. Jin, T. Aida, and S. Inoue, *J. Chem. Soc., Chem. Commun.*, 1260 (1993). Copyright by The Royal Society of Chemistry.

(Bottom right) NANOSENSORS.

This book is printed on acid-free paper. ©

Copyright © 2000 by Academic Press

All rights reserved.

No part of this publication may be reproduced or transmitted in any form or by any means, electronic or mechanical, including photocopy, recording, or any information storage and retrieval system, without permission in writing from the publisher.

The appearance of the code at the bottom of the first page of a chapter in this book indicates the Publisher's consent that copies of the chapter may be made for personal or internal use of specific clients. This consent is given on the condition, however, that the copier pay the stated per-copy fee through the Copyright Clearance Center, Inc. (222 Rosewood Drive, Danvers, Massachusetts 01923), for copying beyond that permitted by Sections 107 or 108 of the U.S. Copyright Law. This consent does not extend to other kinds of copying, such as copying for general distribution, for advertising or promotional purposes, for creating new collective works, or for resale. Copy fees for pre-2000 chapters are as shown on the title pages; if no fee code appears on the title page, the copy fee is the same as for current chapters. \$30.00.

The information provided in this handbook is compiled from reliable sources but the authors, editor, and the publisher cannot assume any responsibility whatsoever for the validity of all statements, illustrations, data, procedures, and other related materials contained herein or for the consequence of their use.

#### ACADEMIC PRESS

A Harcourt Science and Technology Company  
525 B Street, Suite 1900, San Diego, CA 92101-4495, USA  
<http://www.apnet.com>

Academic Press  
24-28 Oval Road, London NW1 7DX, UK  
<http://www.hbuk.co.uk/ap/>

#### Library of Congress Cataloging-in-Publication Data

Nalwa, Hari Singh, 1954-

Handbook of nanostructured materials and nanotechnology / Hari Singh Nalwa.  
p. cm.

Includes indexes.

ISBN 0-12-513760-5

1. Nanostructured materials. 2. Nanotechnology. I. Title.

TA418.9.N35 N32

620'.5-dc21

98-43220

CIP

International Standard Book Number: 0-12-513761-3

Printed in the United States of America

99 00 01 02 03 MB 9 8 7 6 5 4 3 2 1

## Foreword

Nanostructured materials are becoming of major significance and the technology of their production and use is rapidly growing into a powerful industry. These fascinating materials whose dimension range for 1–100 nanometer ( $1 \text{ nm} = 10^{-9} \text{ m}$ , i.e., one billionth of a meter) include quantum dots, wires, nanotubes, nanorods, nanofilms, nanoprecision self assemblies and thin films, nanosize metals, semiconductors, biomaterials, oligomers, polymers, functional devices, etc. etc. It is clear that the number and significance of new nanomaterials and application will grow explosively in the coming twenty-first century.

This dynamical fascinating new field of science and its derived technology clearly warranted a comprehensive treatment. Dr. Hari Singh Nalwa must be congratulated to have undertaken the task to organize and edit such a massive endeavor. His effort resulted in a truly impressive and monumental work of fine volumes on nanostructured materials covering synthesis and processing, spectroscopy and theory, electrical properties, and optical properties, as well as organics, polymers, and biological materials. One hundred forty-two authors from 16 different countries contributed 62 chapters encompassing the fundamental compendium. It is the merit of these authors, their contributions coordinated most knowledgeably and skillfully by the editor, that the emerging science and technology of nanostructured materials is enriched by such an excellent and comprehensive core-work, which will be used for many years to come by all practitioners of the field, but also will inspire many others to join in expanding its vistas and application.

**Professor George A. Olah**  
University of Southern California  
Los Angeles, USA  
Nobel Laureate Chemistry, 1994



# Lecture Notes in Physics

## Editorial Board

R. Beig, Wien, Austria  
 B.-G. Englert, Ismaning, Germany  
 U. Frisch, Nice, France  
 P. Hänggi, Augsburg, Germany  
 K. Hepp, Zürich, Switzerland  
 W. Hillebrandt, Garching, Germany  
 D. Imboden, Zürich, Switzerland  
 R. L. Jaffe, Cambridge, MA, USA  
 R. Lipowsky, Gölz, Germany  
 H. v. Löhneysen, Karlsruhe, Germany  
 I. Ojima, Kyoto, Japan  
 D. Sornette, Nice, France, and Los Angeles, CA, USA  
 S. Theisen, Gölz, Germany  
 W. Weise, Trento, Italy, and Garching, Germany  
 J. Wess, München, Germany  
 J. Zittartz, Köln, Germany

## Managing Editor

W. Beigböck  
 c/o Springer-Verlag, Physics Editorial Department II  
 Tiergartenstrasse 17, 69121 Heidelberg, Germany

## Springer

Berlin  
 Heidelberg  
 New York  
 Barcelona  
 Hong Kong  
 London  
 Milan  
 Paris  
 Tokyo

Centro Ricerche Fiat	
Biblioteca	
Matr.	N. S.
11467	9482

Physics and Astronomy

<http://www.springer.de/phys/>

ONLINE LIBRARY

## The Editorial Policy for Monographs

The series *Lecture Notes in Physics* reports new developments in physical research and teaching - quickly, informally, and at a high level. The type of material considered for publication in the monograph Series includes monographs presenting original research or new angles in a classical field. The timeliness of a manuscript is more important than its form, which may be preliminary or tentative. Manuscripts should be reasonably self-contained. They will often present not only results of the author(s) but also related work by other people and will provide sufficient motivation, examples, and applications. The manuscripts or a detailed description thereof should be submitted either to one of the series editors or to the managing editor. The proposal is then carefully refereed. A final decision concerning publication can often only be made on the basis of the complete manuscript, but otherwise the editors will try to make a preliminary decision as definite as they can on the basis of the available information.

Manuscripts should be no less than 100 and preferably no more than 400 pages in length. Final manuscripts should be in English. They should include a table of contents and an informative introduction accessible also to readers not particularly familiar with the topic treated. Authors are free to use the material in other publications. However, if extensive use is made elsewhere, the publisher should be informed. Authors receive jointly 30 complimentary copies of their book. They are entitled to purchase further copies of their book at a reduced rate. No reprints of individual contributions can be supplied. No royalty is paid on *Lecture Notes in Physics* volumes. Commitment to publish is made by letter of interest rather than by signing a formal contract. Springer-Verlag secures the copyright for each volume.

## The Production Process

The books are hardbound, and quality paper appropriate to the needs of the author(s) is used. Publication time is about ten weeks. More than twenty years of experience guarantee authors the best possible service. To reach the goal of rapid publication at a low price the technique of photographic reproduction from a camera-ready manuscript was chosen. This process shifts the main responsibility for the technical quality considerably from the publisher to the author. We therefore urge all authors to observe very carefully our guidelines for the preparation of camera-ready manuscripts, which we will supply on request. This applies especially to the quality of figures and halftones submitted for publication. Figures should be submitted as originals or glossy prints, as very often Xerox copies are not suitable for reproduction. For the same reason, any writing within figures should not be smaller than 2.5 mm. It might be useful to look at some of the volumes already published or especially if some atypical text is planned, to write to the Physics Editorial Department of Springer-Verlag direct. This avoids mistakes and time-consuming correspondence during the production period.

As a special service, we offer free of charge  $\text{\LaTeX}$  and  $\text{\TeX}$  macro packages to format the text according to Springer-Verlag's quality requirements. We strongly recommend authors to make use of this offer, as the result will be a book of considerably improved technical quality.

For further information please contact Springer-Verlag, Physics Editorial Department II, Tiergartenstrasse 17, D-69121 Heidelberg, Germany.

Series homepage - <http://www.springer.de/phys/books/lnpm>

Stefan Odenbach

# Magnetoviscous Effects in Ferrofluids

 Springer

## Authors

Stefan Odenbach  
Universität Bremen  
ZARM  
Am Fallturm  
28359 Bremen, Germany

Cover picture: by S. Odenbach.

Library of Congress Cataloging-in-Publication Data applied for.

Die Deutsche Bibliothek - CIP-Einheitsaufnahme

Odenbach, Stefan:  
Magnetoviscous effects in ferrofluids / Stefan Odenbach. - Berlin ;  
Heidelberg : New York ; Barcelona ; Hong Kong ; London ; Milan ; Paris ;  
Tokyo : Springer, 2002  
(Lecture notes in physics : N.s. M. Monographs ; 71)  
(Physics and astronomy online library)  
ISBN 3-540-43068-7

ISSN 0940-7677 (Lecture Notes in Physics. Monographs)  
ISBN 3-540-43068-7 Springer-Verlag Berlin Heidelberg New York

This work is subject to copyright. All rights are reserved, whether the whole or part of the material is concerned, specifically the rights of translation, reprinting, reuse of illustrations, recitation, broadcasting, reproduction on microfilm or in any other way, and storage in data banks. Duplication of this publication or parts thereof is permitted only under the provisions of the German Copyright Law of September 9, 1965, in its current version, and permission for use must always be obtained from Springer-Verlag. Violations are liable for prosecution under the German Copyright Law.

Springer-Verlag Berlin Heidelberg New York  
a member of BertelsmannSpringer Science+Business Media GmbH  
<http://www.springer.de>

© Springer-Verlag Berlin Heidelberg 2002  
Printed in Germany

The use of general descriptive names, registered names, trademarks, etc. in this publication does not imply, even in the absence of a specific statement, that such names are exempt from the relevant protective laws and regulations and therefore free for general use.

Typesetting: Camera-ready by the author  
Cover design: design & production, Heidelberg

Printed on acid-free paper  
SPIN: 10862307 55/3141/du - 5 4 3 2 1 0

## Preface

Within the scope of this work we've investigated the magnetoviscous effects – i.e. the changes of viscous properties due to the action of magnetic fields – in so-called ferrofluids. These fluids, suspensions of magnetic nanoparticles in appropriate carrier liquids, show a pronounced increase of viscosity in the presence of moderate magnetic fields with strengths of the order of several tens of mT. Classically this effect is explained by the hindrance of the free rotation of magnetic particles – with a magnetic moment spatially fixed in the particle – in a shear flow due to magnetic torques trying to align the particles' magnetic moments with the magnetic field direction.

Starting from the classical theory by Mark Shliomis (Shliomis, 1972) we've performed a couple of experiments to validate the predictions of the theory. The use of relatively concentrated commercial magnetic fluids lead to the conclusion that the mentioned theory – developed for highly diluted fluids – is not able to give a quantitative description of the behavior of commercial fluids. The discrepancies have been attributed to the appearance of interparticle interactions between the magnetic particles.

Since the microscopic make-up of commercial ferrofluids is relatively complicated, and in particular parameters like the size distribution of the magnetic particles are not known precisely, a theoretical description of the microscopic reasons for the fluids' macroscopic behavior is impossible without further information. Therefore we've started a series of investigations shedding light on the viscous behavior of magnetic fluids in the presence of magnetic fields, stepwise reducing the number of relevant microscopic parameters to prepare a basis for sufficient modeling of concentrated ferrofluids.

As a first step in this development a specialized rheometer for the investigation of magnetic fluids has been designed. With this rheometer, allowing well-defined application of a magnetic field to a rheometric flow of ferrofluids, we've investigated the shear dependence of the magnetoviscous effect in commercial ferrofluids. These investigations showed that the field-dependent increase of viscosity reduces with increasing shear rate. On the basis of this result we developed a model, assuming that the formation of chains of magnetic particles dominates the magnetoviscous properties of magnetic fluids. The chains themselves represent large magnetic structures which lead to pronounced changes of viscosity if a field is applied. Furthermore, the rupture of the chains in a shear flow and the resulting reduction of the size of the magnetic structures is a starting point for the explanation of the observed shear thinning.

Since chains of magnetic particles can only be formed by particles exhibiting a sufficient interparticle interaction, and since this interaction depends furthermore

on the size of the particles, the next step had to be a clarification, whether the relatively small fraction of large particles in the suspension used is of major importance for magnetoviscosity in ferrofluids. These large particles exhibit – in contrast to the majority of particles with diameters of about 10 nm – sufficiently strong interaction to explain at least the appearance of chain formation.

To get an insight into these questions, we've performed experiments using ferrofluids with variable contents of large particles. In these experiments it was clearly shown that the magnetoviscous effect rises with an increasing amount of large particles. This leads to further input for the theoretical modeling. In an extended approach the ferrofluid is assumed to be a bidisperse system containing a large fraction of small particles, which do not directly contribute to magnetoviscosity, and a small fraction of large particles which form chains determining the field-dependent changes of viscosity. On the basis of these assumptions the magnetoviscous properties could be fitted quantitatively to the experimental data using methods of statistical physics. Thus, a first quantitative description of the microscopic reasons for the rheological behavior of ferrofluids was found, taking into account the effects to the formation of magnetic particle chains. The conclusion that chains exist in the fluids gives rise to the assumption that these fluids should exhibit viscoelastic effects too. To prove this, we finally carried out experiments on the Weissenberg effect, i.e. the climb of a free surface of magnetic fluids at a rotating axis, showing the field-dependent existence of normal stress differences in ferrofluids. Again, the experimentally found behavior could be explained by the formation and rupture of chains of magnetic particles in the fluid.

Thus – within the scope of this work – we've been able to develop a microscopic model of ferrofluids allowing a quantitative description of their rheological behavior, and to prove this model with numerous experimental results on field-dependent effects in ferrofluids rheology. On the basis of these results, information for the optimization of ferrofluids with respect to their magnetoviscous behavior can be obtained, leading to the synthesis of new ferrofluids. Such fluids with enhanced magnetoviscous properties may be used in the future development of devices using the magnetically induced control of viscous properties as an active part in technical applications like dampers or clutches.

Investigations like those described in this work require not only a certain time span to be performed but also the help and cooperation of numerous colleagues and the financial support enabling the research activities.

Thus I'd like to take the opportunity to express my gratitude to those helping me to do this research during recent years.

First of all I've to thank Prof. Dr.-Ing. H. J. Rath and Prof. Dr. K. Stierstadt for providing me with a working environment in Bremen as well as in former times in Munich that gave me the possibility of developing ideas and building up a research team able to explore this new and interesting field. Without these boundary conditions this wouldn't have been possible.

Furthermore my gratitude goes to my co-workers who were prepared to work even in difficult ways towards new scientific and technical goals: Dipl. Phys. H. Gilly for lively discussions during the time in Munich, Dipl. Phys. H. Störk who

built the first version of the ferrofluid rheometer in Wuppertal, and last but not least the members of the ZARM-ferrofluid team who participated in various experiments which led to the results presented, Dipl.-Ing. J. Fleischer, Dipl.-Ing. M. Heyen, Dipl.-Ing. K. Melzner, Dipl.-Ing. T. Rylewicz, Dipl.-Ing. S. Thurm and Dipl.-Ing. T. Völker.

Besides this I'm grateful to numerous colleagues and friends for fruitful and enlightening discussions. In this case it's nearly impossible to name all those who have been with me during the years, but I'd like to mention particularly: Prof. E. Blums, Prof. A. Zubarev and Prof. L. Vekas who were our guests in Bremen numerous times in the course of fruitful cooperations; Dr. K. Raj who provided us with the fluid series for the experiments concerning the influence of large particles; Prof. K. Stierstadt, Dr. H. W. Müller and Dipl.-Ing. Ch. Eigenbrod who helped me with deep and inspiring discussions; and numerous members of the German ferrofluid community who are helping to form a powerful research community on magnetic fluids.

As mentioned, financial support is also essential for the performance of research in general. In this respect I'd like to mention particularly the Deutsche Forschungsgemeinschaft (DFG) for granting most of the experimental work performed during the years in Bremen. In this context I'd like to express my gratitude to Dr. W. Lachenmeier from DFG for the excellent cooperation during the establishment of the DFG priority program on magnetic fluids focusing partly on the topics discussed here. Furthermore I've to thank the Deutsches Zentrum für Luft- und Raumfahrt (DLR), in particular Dr. H. Binnenbruck, for financial support over many years. In addition, the flight opportunities provided by DLR and ESA were of essential importance for the Weissenberg-effect experiments.

Since most of the work presented has an experimental character, the technical support provided by the workshop at ZARM and the Fallthum Betriebsgesellschaft was often of great importance to the success of our research. I'm especially grateful for this, since we often had to set extremely tight deadlines which were always observed.

Besides all the research work, these pages had finally to be written, and in this context I'd like to express my thanks to E. Renschen and C. Wiese for a lot of typing.

In general, the development of scientific activities is a part of life that can not be successful if it is not supported by an appropriate private environment. Many of the colleagues mentioned above have become real friends during the years, supporting me even in difficult times.

But particular gratitude in this respect goes to my parents and my wife Marlene, supporting me over all the years and understanding the difficulties and setbacks of this kind of life.

Bremen, 2001

*Stefan Odenbach*

## Contents

1. Introduction .....	1
1.1 Magnetic fluids .....	1
1.2 Magnetoviscous effects .....	2
1.3 Publications on ferrofluids .....	3
1.4 The scope of this work .....	4
2. Magnetic fluids .....	7
2.1 Basic structure and stability .....	8
2.2 Magnetic properties of ferrofluids .....	14
2.2.1 Equilibrium magnetization .....	14
2.2.2 Relaxation of magnetization .....	20
2.3 Viscous properties in the absence of magnetic fields .....	22
2.4 Applications of magnetic fluids .....	26
2.4.1 Mechanical applications .....	26
2.4.2 Thermal applications .....	27
2.4.3 Medical applications .....	28
2.4.4 Aspects for the design of future applications .....	29
2.4.5 Applications and the magnetoviscous effect .....	31
3. The magnetoviscous effect in highly diluted ferrofluids .....	33
3.1 Rotational viscosity .....	35
3.2 "Negative" viscosity .....	52
4. Magnetoviscosity in concentrated ferrofluids .....	59
4.1 Magnetoviscous effects in commercial fluids at high shear rate .....	59
4.2 Experimental techniques for the investigation of magnetoviscous properties in ferrofluids .....	62
4.2.1 Capillary viscometers .....	62
4.2.2 Rheometers .....	64
4.2.3 A specialized rheometer for the study of magnetoviscous effects in ferrofluids .....	68
4.3 Shear dependence of the magnetoviscous effect .....	78
4.3.1 Results for a commercial ferrofluid and a first approach to a microscopic explanation .....	78
4.3.2 Experimental results for fluids with different microscopic make-up .....	85

4.3.3 Controlled change of the microscopic make-up of commercial ferrofluids.....	93
4.3.4 Microscopic explanation of magnetoviscosity in fluids with interparticle interaction .....	96
4.3.5 Rheological description of magnetoviscosity .....	102
4.4 Viscoelastic effects in ferrofluids .....	107
4.4.1 Normal stress differences in magnetic fluids .....	108
5. Magnetorheological Fluids .....	123
5.1 Definition and basic properties of magnetorheological fluids .....	123
5.2 Viscous properties of magnetorheological fluids .....	125
5.3 Future development in magnetorheology .....	127
6. Conclusion and outlook .....	131
Appendix A .....	135
List of symbols.....	137
References.....	143

## 1. Introduction

### 1.1 Magnetic fluids

Fluids which can be effectively controlled by magnetic fields of moderate strength are a challenging subject for scientists interested in the basics of fluid mechanics as well as for application engineers. For the basic research the introduction of a controllable force into the fundamental hydrodynamic equations opens a fascinating field of new phenomena.

Forces which can be varied over wide ranges in strength and direction relative to a flow are usually only applicable in theoretical treatments. For forces exhibited by magnetic field gradients the situation changes since magnetic fields can be varied quite well in strength and direction using different types of coils, pole shoes and permanent magnets. If the magnetic influence exerted by a magnetic field becomes strong enough to compete with gravitational forces, a new class of hydrodynamic phenomena becomes experimentally accessible.

Also the design of applications using fluids as relevant active or passive components gains new possibilities if the fluids can be positioned or moved by a force which can be produced by an electric current through a coil being controlled and switched electronically. Again - if the necessary forces can be produced by moderate fields which are generated with a relatively small technical effort - new design ideas using an additional control parameter can be realized.

Due to the fact that no natural liquids offer these features, the starting point of the field of magnetic fluid research can be found in theoretical treatments of magnetically controlled heat transfer machines (Resler and Rosensweig, 1964). Since these early ideas already showed that a liquid material with controllable magnetic properties would provide numerous development possibilities, strong efforts have been undertaken to synthesize a system enabling the mentioned magnetic control.

As will be shown later on, suspensions of magnetic nanoparticles in appropriate carrier liquids are a sufficient realization of such a new class of smart materials. What the first theoretical ideas predicted, the experiments have confirmed. Several hundred scientific publications per year and thousands of approved patents document the vitality of ferrofluid research as well as the close connection to applied engineering.

But not only engineers, experimental and theoretical physicists contribute to the development of the field called ferrohydrodynamics (Neuringer and Rosen-

sweig, 1964). The complexity of the system and its difficult chemical make-up require distinct knowledge in chemistry and colloidal physics to synthesize new and improved liquids and to modify the basic properties of the suspensions. Moreover the utilization of the system is not only restricted to technical applications – a use is also possible for various medical treatment purposes. Thus, the overall field of ferrofluid research has a highly interdisciplinary character, bringing chemists, experimental physicists, engineers, theoretical physicists, applied mathematicians and physicians together.

The interdisciplinarity of the field leads to the necessity for strong cooperation between scientists from different research directions. In principle, basic research has to provide information about the relation between the microstructural make-up and the macroscopic field-dependent properties of the liquids. This knowledge has to be used to tailor special suspensions for new application ideas defining certain requests concerning the fluids behavior in the presence of magnetic fields. Obviously such an interconnected research forces a mutual fertilization of the involved research areas, making the whole field highly challenging from a scientific point of view.

The future development perspective and this interdisciplinary aspect has been the driving force in the establishment of various national research programs, e.g. in Japan and France. The most recent of these programs, a DFG priority program started in Germany in 2000, accounts especially for the interdisciplinarity of the field by combining the efforts of chemists and basic researchers with application engineers and scientists from medical research fields.

These programs are actually leading to a new concentration of efforts in the field, where the investigation of magnetoviscous effects is one of the core points of interest.

## 1.2 Magnetoviscous effects

Shortly after the publication of the first patent on the synthesis of stable suspensions of nanosized magnetic particles intense research efforts were started in the field, leading to the development of a theoretical background – the theory of ferrohydrodynamics based on early papers by M. Shliomis (Zaitsev and Shliomis, 1969; Shliomis, 1972) – as well as to patents for numerous applications which partly gained commercial importance forcing further development of the whole research area. While basic research covered nearly all areas of flow control and property changes in the fluids induced by the action of magnetic fields, commercially successful applications just used the possibility of the magnetic positioning of the liquids.

The principally predicted employment of the magnetic control of flow in the fluid, or the change of its properties under the influence of a field did not reach the stage of experimental realization since they require relatively high concentration of the suspended magnetic material to achieve a reasonable strength of the effects. The high concentration leads to an interaction of particles, which can not be neglected. The need to account for the interparticle interaction increases the com-

plexity of the system essentially. Thus a well-founded understanding of phenomena observed in such suspensions is relatively hard to obtain. Nonetheless the knowledge about the microstructural properties and their importance for the fluids' macroscopic behavior is the background needed to synthesize application tailored suspensions and to design new devices based on magnetic liquids. Furthermore the influence of magnetic fields on changes in the microstructure of fluids of different make-up has to be taken into account in the prediction of their macroscopic properties.

These problems are of principal importance for the magnetically induced changes in the viscosity of magnetic fluids. The basic theories – formulated nearly three decades ago – model the microstructural make-up of the suspensions in an idealized way, neglecting any kind of interparticle interaction. Therefore these theories can only be used for quantitative predictions of the behavior of highly diluted fluids. In contrast "the promise of controllable fluids", as J.D. Carlson (Carlson, 1994) named the development of new applications of magnetorheological fluids, always requires highly interacting systems to obtain an order of magnitude of the relevant effects – e.g. the magnetoviscous effect – required for commercial needs.

Experimentally it has been found that relatively strong field influence on viscosity can be induced not only in magnetorheological fluids, but also in ferrofluids with sufficient particle-particle interaction. But only recently a deeper understanding of these interactions led to microscopic models quantitatively explaining the experimentally found phenomena. This knowledge is actually used to find ways to optimize the magnetorheological effects in long-term sedimentation stable ferrofluids.

In this context new research concepts have been set up to accelerate the development process. Synthesis of the fluids, basic understanding of their properties, and the development of applications using magnetoviscous properties of the fluids are no longer addressed as isolated research fields. Moreover, programs have been established combining the expertise of the different fields of knowledge in ferrofluid research. The mentioned priority program of DFG is an example of such an integrated research activity. Fluids produced by several synthesizing groups are characterized and rheologically tested and from the understanding of the fluids' behavior steps towards optimization are undertaken. Parallel to this development new applications are designed, using in the beginning existing magnetorheological fluids to define the necessary properties of the fluids to be developed, and thus provide a guideline for the further synthesis steps.

## 1.3 Publications on ferrofluids

As already mentioned, the field of ferrofluid research is actually more than 30 years old. Thus it is clear that not only original publications in journals or conferences have been released, but also textbooks have been published giving overviews on certain areas of the investigation of fluids containing magnetic nanoparticles. In 1985 the famous book "Ferrohydrodynamics" by Ronald Rosensweig

(Rosenzweig, 1985) was issued, and it is still the standard textbook for people entering the field of magnetic fluid research. Rosenzweig's book leads the reader through all areas of the research field – from the synthesis and properties of magnetic fluids and the foundation of the theory of ferrohydrodynamics towards problems of experimental hydrodynamics in ferrofluids as well as the description of various applications. It features examples for flow control and magnetically driven surface and transport instabilities as well as some remarks concerning field-induced changes of the properties of the fluids.

Looking to magnetoviscous effects only the first results of McTague (McTague, 1969) and Rosenzweig (Rosenzweig et al., 1969) are briefly mentioned, and a glance at the related theory by Shliomis (Shliomis, 1972) is given.

A slightly more detailed treatment of the rheology of ferrofluids in a magnetic field was given in the second general textbook on "Magnetic Fluids" by Blums, Cebers and Maiorov (Blums et al., 1997). They include an extended theoretical discussion of rotational viscosity and deal also with questions like the dependence of the magnetoviscous effects on particle shape and the effect of variation of shear rate for weak shear. In addition this book also gives a good overview on ferrofluid research enlightening the related question from a more theoretical point of view.

Besides these two books no general treatment of the whole area of ferrofluid research is currently available. All other books have been published with a focus on certain sub-areas and refer to Rosenzweig and Blums for the general questions. The field of heat and mass transfer was well treated by Blums, Mikhailov and Ozols in "Heat and Mass Transfer in MHD Flows" (Blums et al., 1986) which contains a special section on heat and mass transfer effects in ferrofluids – while the main part of the book is devoted to conducting fluids and thus to the action of Lorentz forces rather than of magnetic body forces.

Furthermore two books on applications of magnetic fluids are available. "Magnetic Fluids and Applications Handbook" by Berkovsky and Bashitovoy (Berkovsky and Bashitovoy, 1996) and "Engineering Applications of Magnetic Fluids" (Berkovsky et al., 1993) give an overview on numerous kinds of usage of ferrofluids in different fields, for example mechanical positioning, separation or even medicine. Besides the mentioned books, further monographs are available in Russian, Berkovsky and Polevikov's work on "Numerical Experiments in Ferrofluids" (Berkovsky and Polevikov, 1988). But since these have not been translated into English, the availability of the information contained is unavailable for an English-speaking reader, reducing their importance and rating.

## 1.4 The scope of this work

With the present work the field of magnetoviscous properties of ferrofluids will be addressed. As mentioned above, the standard textbooks give only a short treatment of the early findings concerning field effects on the rheological behavior of ferrofluids. Moreover no special treatment of this subject has existed till now. On the other hand the investigation of field-induced changes of the viscosity of suspensions of magnetic nanoparticles is one of the most vital areas in magnetic fluid

research nowadays. The current research questions, focusing on the tailored design of fluids for new applications using the magnetoviscous effects, require a detailed understanding of the effect itself as well as of the influence of the microscopic make-up of the fluid on its macroscopic behavior. Since especially the latter mentioned question of the dependence of macroscopic effects on microscopic properties is based on experimental and theoretical results we obtained recently, no comprehensive description of the field exists yet.

So the idea of this work is to combine a description of the basics of magnetoviscous effects with a compilation of the most recent findings on the influence of structure formation on the viscosity of ferrofluids. To achieve this goal, the present work is organized in the following way.

Chapter 2 will introduce the material which is the focus of the discussion. Ferrofluids and their basic properties will be discussed to an extent that allows us to read the upcoming treatment of magnetoviscosity without further basic knowledge on suspensions of magnetic nanoparticles. Besides the discussion of basic properties, Chap. 2 will also contain a short glance on applications of ferrofluids. This part is thought to motivate the engineering aspect of the whole research field in general as well as to highlight the investigation of magnetoviscous effects for applications. This section does not claim to replace the standard textbooks mentioned in Sect. 1.3. Its scope is only to introduce those topics needed for the discussion of the main focus of this work. Thus a couple of references to the standard books are given to enable the reader to find more detailed information on topics from the field of ferrofluid research outside the focus of this work.

In Chap. 3 the basic phenomenon of rotational viscosity, i.e. the influence of a magnetic field on the viscosity of a suspension of noninteracting nanoparticles is discussed. Starting from an explanation of the basic physical background of the phenomena of field-induced viscosity changes in ferrofluids, the theoretical approach of Shliomis is reviewed. Particular interest is paid here to all aspects related to experimental proofs of the theory rather than to a deep theoretical discussion of the approach itself. Nonetheless, the derivation of the basic equation for rotational viscosity is briefly compiled to give the reader a general glance at one of the most fundamental theoretical developments of ferrohydrodynamics. Starting from the various theoretical predictions, experimental proofs of the theory are presented, leading to a discussion of the range of validity of the theory and in particular of the problems that appear if concentrated fluids are considered. Finally, for reasons of completeness, the phenomenon of viscosity reduction in alternating magnetic fields is briefly discussed to illustrate the wide range of phenomena based on the interaction of the magnetic field with the magnetic moment of the particles.

The magnetoviscous effects in concentrated suspensions, and thus in systems of interacting particles, are then discussed in Chap. 4. The starting points for this discussion are the discrepancies found in Chap. 3 in the comparison of Shliomis' theory with the experimental results for concentrated suspensions. Again the experimental investigation of magnetoviscous effects is the center of the discussion. The necessary experimental techniques, and the connected experimental problems are described in detail to form the basis for the discussion of the measured phe-

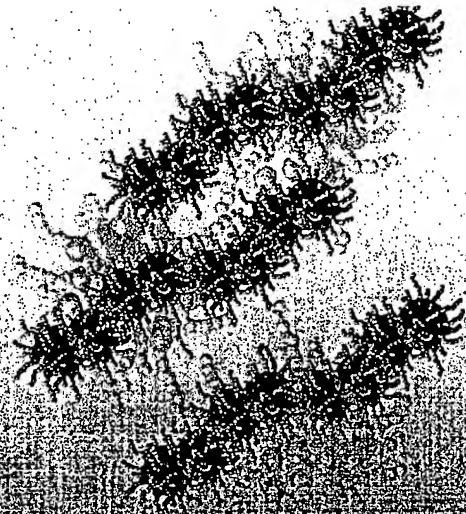


Odenbach  
Magnetoviscous Effects in Ferrofluids

Suspensions of magnetic nanoparticles or ferrofluids can be effectively controlled by magnetic fields, which opens up a fascinating field for basic research into fluid dynamics as well as a host of applications in engineering and medicine. The introductory chapter provides the reader with basic information on the structure and magnetic and viscous properties of ferrofluids. The bulk of this monograph is based on the author's own research activity and deals with ferrohydrodynamics, especially with the magnetoviscous effects. In particular, the author studies in detail the interparticle interactions so far often neglected but of great importance in concentrated ferrofluids. The basic theory and the most recent experimental findings are presented, making the book interesting reading for physicists or engineers interested in smart materials.

Stefan Odenbach

# Magnetoviscous Effects in Ferrofluids



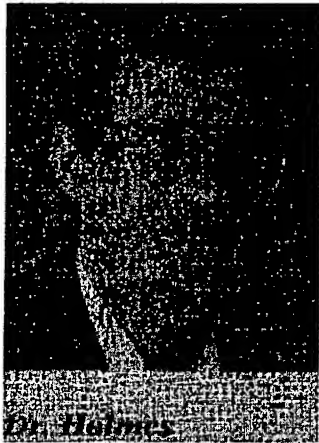
Odenbach, Stefan Magnetoviscous Effects in Ferrofluids

ISSN 0940-7677

ISBN 3-540-43068-7



## Dr Andrew Holmes



### **BIOGRAPHY**

Andrew S Holmes MA PhD MIEE MIEEE

Andrew Holmes obtained the BA degree in physics from Cambridge University in 1987, and the PhD degree in electrical engineering from Imperial College London in 1992. He was a Research Associate in the Department of Electrical and Electronic Engineering, Imperial College London, from 1991 to 1993, when he took up a joint Research Fellowship in Microengineering with Imperial and the Rutherford Appleton Laboratory. He was appointed to a Lectureship at Imperial College London in 1995, and has been a Senior Lecturer there since 2000. Dr Holmes has worked in the areas of optical signal processing, integrated optics and MEMS (micro-electro-mechanical systems), and has published around 65 papers in these areas. His current research interests include fabrication processes based on metal electroforming, applications of laser processing in MEMS manufacturing, micro-assembly techniques, and devices for micro-power generation.

### **RESEARCH PUBLICATIONS**

The full technical presentations of some papers are available on-line. These papers have clickable links, which point to Adobe Portable Display Format (PDF) files. To view or print these files, you must have Adobe Acrobat Reader please click on the icon below and you will be able to download a free copy



#### **1989**

Holmes A.S., Syms R.R.A. "Self-aligning guided wave system for delay line signal processing" SPIE Proceeding 1120, (1989)

Holmes A.S., Lewandowski J., Syms R.R.A., "A Self aligning guided wave optics breadboard", IEE Colloquium on Integrated Optics, London, 6 June (1989) [Get PDF](#)

#### **1991**

Birmingham, March 29th (2000) [Get PDF](#)

**2001**

Fieret J., Holmes A.S., Paineau S., Quentel F., "Multilevel diffractive optical element manufacture by excimer laser ablation using half-tone masks", presented at SPIE Photonics West LASE 2001, San Jose, CA, USA, 19-26 Jan (2001) [Get PDF](#)

Wang C.H., Holmes A.S., "Laser-assisted bumping for flip chip assembly", IEEE Trans-Electronic Packaging Manufacturing, 24 (2), 109-114 (2001) [Get PDF](#)

Holmes A.S., "Laser fabrication and assembly processes for MEMS", presented at SPIE Photonics West LASE 2001, San Jose, CA, USA, 19-26 Jan (2001) [Get PDF](#)

Holmes A.S., "Laser processes for MEMS manufacture", 2nd International Symposium on Laser Precision Microfabrication 2001 (LPM2001), Singapore, 16-18 May 2001 [Get PDF](#)

**2003**

Stassen I., Fieret J., Holmes A.S., Lee K.W., "CAD/CAM software for an industrial laser micro-manufacturing tool", SPIE Proceedings vol. 4977, Proc. Photonics West LASE 2003, San Jose, USA, 25-31 Jan 2003, 198-206. [Get PDF](#)

Hong G., Holmes A.S., Heaton M.E., "SU8 resist plasma etching and its optimisation", Proc. Symp. on Design, Test, Integration and Packaging (DTIP) of MEMS/MOEMS, Mandelieu - La Napoule, France, 5-7 May 2003, 268-271. [Get PDF](#)

Hong G., Holmes A.S., Heaton M.E., Pullen K.R., "Design, fabrication and characterization of an axial-flow turbine for flow sensing", Proc. Transducers '03, Boston MA, USA, 8-12 June 2003, 702-705. [Get PDF](#)

Holmes A.S., Heaton M.E., Hong G., Pullen K.R., Rumsby P.T., "Laser profiling of 3-D microturbine blades", SPIE Proc. Vol. 5063, Proc. 4th International Symposium on Laser Precision Microfabrication (LPM2003), Munich, Germany, 21-24 June 2003, 152-156. [Get PDF](#)

Mitcheson P.D., Miao P., Stark B.H., Holmes A.S., Yeatman E.M., Green T.C., "Analysis and optimisation of MEMS electrostatic on-chip power supply for self-powering of slow-moving sensors", Proc. Eurosensors XVII, Guimarães, Portugal, 21-24 Sept 2003, 48-51. [Get PDF](#)

**Accepted & Submitted Papers**

Mitcheson P.D., Green T.C., Yeatman E.M., Holmes A.S., "Architectures for vibration-driven micro-power generators", IEEE/ASME J. Microelectromechanical Systems, in press.

Holmes A.S., "Excimer laser micromachining with half-tone masks for the fabrication of 3D microstructures", IEE Proc. – Sci. Meas. & Technol., in press.

Yates D.C., Holmes A.S., Burdett A.J., "Optimal transmission frequency for ultra-low power short-range radio links", IEEE Trans. Circ. & Syst. I – Fundamental Theory & Applications, in press.

George D.S., Onischenko A., Holmes A.S., "On the angular dependence of focussed laser ablation by nanosecond pulses in solgel and polymer materials", Applied Physics Letters, in press.

Hong G., Holmes A.S., Heaton M.E., "SU8-plasma etching and its optimisation", Microsystem Technologies, accepted for publication.

Holmes A.S., Hong G., Pullen K.E., "Axial-flux, permanent magnet machines for micro-power generation", IEEE/ASME J. Microelectromechanical Systems, submitted.

Miao P., Holmes A.S., Yeatman E.M., Green T.C., Mitcheson P.D., "Micro-machined variable capacitors for

# Multilevel diffractive optical element manufacture by excimer laser ablation and halftone masks

F. Quentel<sup>a\*</sup>, J. Fieret<sup>b\*\*</sup>, A. S. Holmes<sup>c\*\*\*</sup> and S. Paineau<sup>a\*\*\*\*</sup>.

<sup>a</sup>Thomson-CSF, Central Research Lab ; Domaine de Corbeville, 91404 Orsay, France.

<sup>b</sup>Exitech Ltd ; Handborough park, Long Handborough, Oxford OX8 2LH, United Kingdom.

<sup>c</sup>Imperial College, Optical & Semiconductor Devices Group, Department of Electrical & Electronic Engineering ; Exhibition Road, London SW7 2BT, United Kingdom.

## ABSTRACT

A novel method is presented to manufacture multilevel diffractive optical elements (DOEs) in polymer by single-step KrF excimer laser ablation using a halftone mask. The DOEs have a typical pixel dimension of 5  $\mu\text{m}$  and are up to 512 by 512 pixels in size. The DOEs presented are Fresnel lenses and Fourier computer generated holograms, calculated by means of a conventional iterative Fourier transform algorithm. The halftone mask is built up as an array of 5  $\mu\text{m}$ -square pixels, each containing a rectangular or L-shaped window on an opaque background. The mask is imaged onto the polymer with a 5x, 0.13 NA reduction lens. The pixels are not resolved by the lens, so they behave simply as attenuators, allowing spatial variation of the ablation rate via the window size. The advantages of halftone mask technology over other methods, such as pixel-by-pixel ablation and multi-mask overlay, are that it is very fast regardless of DOE size, and that no high-precision motion stages and alignment are required. The challenges are that the halftone mask is specific to the etch curve of the polymer used, that precise calibration of each grey-level is required, and that the halftone mask must be calculated specifically for the imaging lens used. This paper describes the design procedures for multilevel DOEs and halftone masks, the calibration of the various levels, and some preliminary DOE test results.

**Keywords:** 3D-Micromachining, excimer laser ablation, halftone mask, diffractive optical elements.

## 1 INTRODUCTION

DOEs can be found in an increasing number of applications involving lasers, for example optical computation, optical interconnects, DVD optical pick up systems and mux/demux devices for telecommunications. Their interest lies in their ability to encode any phase profile and hence to implement optical functions unachievable by use of conventional optics. In addition, they offer the advantage of being thin, planar and light-weight elements that can easily be integrated in larger systems.

Several techniques exist for the fabrication of multilevel DOEs. We can classify them in two categories: raster scanning techniques and mask-based or batch methods.

Electron beam writers and focused laser beam writers are the two main raster fabrication tools<sup>1,2</sup>. In both cases, the beam is scanned over the sample according to the geometry of the desired structures. By varying the energy dose at the substrate, different relief levels can be obtained. In serial laser writing the beam is usually focused onto the surface of a photosensitive material (e.g. photoresist) on a specific substrate. After exposure, the photosensitive layer is developed to yield a 3D surface profile which can be transferred into the underlying substrate by etching. With an electron-beam pattern generator, the process is similar, except that two raster writing schemes are possible: focused beam writing and variable shaped beam writing. In the latter case, the beam is imaged on the substrate with a shape that can be varied dynamically during the process.

\* [quentel@lcr.thomson-csf.com](mailto:quentel@lcr.thomson-csf.com) ; phone +33 (0)1 69 33 92 26 ; fax : +33 (0)1 69 33 08 62 ;

\*\* [j.fieret@exitech.co.uk](mailto:j.fieret@exitech.co.uk) ; phone +44 1993 883324; fax +44 1993 883334 ;

\*\*\* [a.holmes@ic.ac.uk](mailto:a.holmes@ic.ac.uk) ; phone +44 (0)20 7594 6239 ; fax +44 (0)20 7823 8125 ;

\*\*\*\* [paineau@lcr.thomson-csf.com](mailto:paineau@lcr.thomson-csf.com) ; phone +33 (0)1 69 33 92 28 ; fax +33 (0)1 69 33 08 62.

Excimer laser raster micro-machining of polymers has also been reported<sup>3,4</sup>. Since the excimer laser beam cannot be focused due to its poor beam quality, it is imaged through a mask to produce an elementary figure which defines a single pixel on the substrate. Thanks to the photo-ablation process, no development step is needed.

In comparison with laser writing, electron-beam writing is capable of producing smaller feature sizes (of the order of several hundreds of nanometers) but it is also much more expensive. In both cases, continuous relief fabrication is possible. However, they both can only produce one element at a time and the time required to produce large DOEs can be very long. As a consequence, raster scanning systems are confined to prototyping of DOEs.

As opposed to serial writing systems, mask-based technologies can, and have been used for batch manufacturing of DOEs. Most of them stem directly from the VLSI techniques used in microelectronics. Thus, conventional binary mask photolithography has been successfully applied for multilevel DOEs fabrication. M binary chrome-on-quartz masks can produce  $2^M$  relief levels by means of successive photoresist spinning, exposure and development steps. Although this method enables high quality DOEs to be fabricated, it is limited by the alignment accuracy of the mask aligner when the critical dimension of the DOE becomes less than a micron or so. Besides, successive mask alignment and associated processes make it a complex and expensive technique.

Novel mask-based techniques have been developed to overcome these limitations while keeping the advantage of parallel processing. For example, conventional lithography using either greyscale or half-tone masks can produce 3-dimensional micro-optical elements within a single lithographic process. Half-tone masks are binary masks in which the critical dimension is smaller than the resolution limit of the optical exposure system. Continuous profiles are achievable through this technique<sup>5,6,7</sup>. Most half-tone masks are designed for use with a projection lens, where the resolution requirements are lower at the mask plane than at the workpiece.

Greyscale lithography is a very similar approach for direct 3-dimensional fabrication of diffractive elements<sup>8</sup>. This technique is based on HEBS or LDW glass masks which are true grey level masks. Grey levels are encoded in the mask by local reduction of silver ions present in a thin layer at the surface of the mask. In comparison to half-tone masks, greyscale masks are more expensive. However they do offer higher resolution because the features determining the local transmission of the mask are of atomic scale. For this reason, greyscale masks can be used in contact mode (rather than projection mode), which makes the process simpler and avoids possible defocusing errors.

In this paper we present a novel technology for multi-level structures manufacturing. First results are presented in the field of DOE micro-machining. The technique is based on laser ablation through a chrome-on-quartz half-tone mask with a demagnifying high NA lens. This approach combines the advantages of half-tone masks (i.e. reduction of the steps involved for 3D micromachining and improved cost-effectiveness) with the simplicity of laser ablation process. Indeed there is no development step required in the method. As with normal projection lithography, only a portion of the mask can be processed at one time. Nevertheless it is a fast, cheap and high-quality method for small scale fabrication of DOEs.

Section 2 describes in detail the fabrication system and the associated half-tone mask technology. Process characterization for different polymers is presented in section 3. Finally, in section 4, the technique is applied to multilevel DOE manufacturing and some first results are given.

## 2 DESCRIPTION OF THE FABRICATION SYSTEM

### 2.1 Laser Workstation

The laser system used is an Exitech 8000 series excimer laser workstation. The laser is a KrF excimer laser operating at 248 nm. The energy per pulse is typically equal to 0.5 J, although only a small fraction of the available energy is generally used. The pulse duration is approximately 20 ns, and the maximum repetition rate is 100 Hz. Because the intensity profile of an excimer laser output is quite non-uniform, beam forming optics and a beam homogenizer are used to produce a uniform intensity field at the mask plane. The mask plane is imaged on the substrate to be ablated with 5x demagnification by a 0.13 NA Microlas UV objective, which has a 18 mm diameter image field. The mask is positioned by means of large, linear motor driven Aerotech translation stages. The mask holder can handle several masks of different sizes at the same time. The substrate is positioned at the image plane of the lens by means of similar Aerotech stages (see Figure 1).

This workstation is capable of synchronized scanning of the mask over the substrate. Thus a complete and large layout on the mask can be transferred to the substrate simply by continuously displacing the mask and the substrate in opposite directions. For a 5x demagnification introduced by the lens, the substrate stage should travel at a speed one-fifth that of the

mask one. Such a technique enables a transfer of any layout having dimensions much larger than the laser beam section. Since the process is continuous, stitching errors as encountered with a step and repeat approach are avoided.

For our purpose, synchronized scanning is not necessary. Indeed the largest DOEs present on the mask have smaller dimensions than the object field of the lens and the laser beam size. DOEs ablation is therefore achieved statically after the mask has been positioned at the right position.

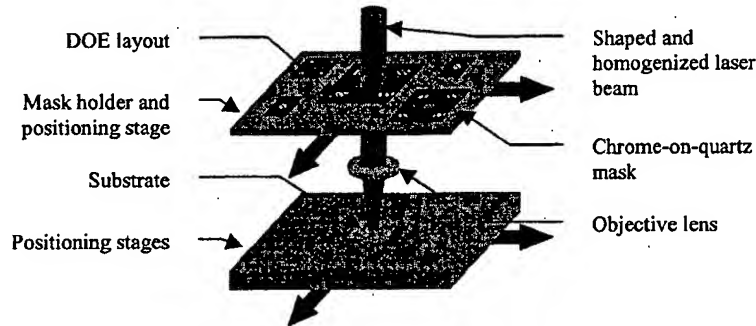


Figure 1 : diagram of the laser workstation

The micro-fabrication technique we present in this paper does not require high precision positioning stages. Three dimensional reliefs are realised within a single step thanks to the half-tone mask, and so consecutive binary masks do not have to be precisely positioned over the substrate. Furthermore, provided the lens used has a sufficiently large field for imaging an entire DOE layout, the mask does not have to be translated during the exposure process. Stage displacements are then required only for selecting a new layout on the mask and for travelling to a new processing position on the substrate.

The laser fluence on the substrate can be varied by means of an attenuator located in the laser path. For changing the ablation characteristics the number of laser pulses can also be varied. All the components of the laser workstation are computer controlled.

## 2.2 Half-tone masks

Half-tone masks are binary masks that achieve a greyscale effect (i.e. offer multiple transmission levels) when used in conjunction with an appropriate optical system. The transmission of a chrome-on-quartz mask can be modulated by creating a pattern of transparent small apertures in the chrome layer. These apertures should be small enough not to be transferred on the workpiece, which means they must have dimensions below the resolution limit of the optical exposure system used.

Such an arrangement of clear apertures can modulate the transmission by two mechanisms: pulse-width modulation (PWM) and pulse density modulation (PDM). In PWM, the aperture pitch is constant all over the mask, while the aperture size is variable. In PDM, the apertures are of fixed size but their pitch can vary.

The half-tone mask used in this study was manufactured on a chrome-on-quartz mask plate. It relies on pulse width modulation and consists of a two-dimensional array of small unit cells of fixed size, with the variation in transmission being obtained by creation of a window of appropriate size in the chrome layer of each cell. The overall transmission (including all diffracted orders) is thus the window area divided by the unit cell area.<sup>9</sup>

Any region of the mask will behave as a 2-D diffraction grating and, in order for the mask to behave simply as an attenuator, only the zeroth diffraction order of this grating should pass through the optical system; otherwise the half-tone pattern will produce unwanted fine-structure on the workpiece. For coherent illumination, the condition for rejection of the first and higher orders is:

$$p < \frac{\lambda}{NA} \times M \quad (1)$$

where  $p$  is the pitch of the half-tone pattern,  $\lambda$  is the illumination wavelength, NA is the numerical aperture of the projection lens, and  $M$  is its demagnification. This ignores the partially coherent nature of the mask illumination in the laser workstation, but is nevertheless a useful guide. With only the zeroth order passing through the system, the transmitted power varies as the square of the chrome-free fraction of the unit cell.

The lens used in this work was a 0.13 NA Microlas lens capable of 5x demagnification. According to equation 1, for a wavelength of 248 nm (KrF laser), the maximum half-tone pitch for this lens is 9.5  $\mu\text{m}$ . In fact the mask was designed as an array of 5  $\mu\text{m}$  x 5  $\mu\text{m}$  square chrome unit cells each containing a rectangular or L-shaped clear window.

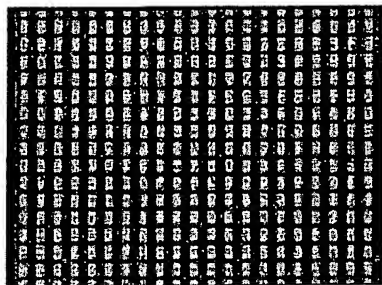


Figure 2 : Picture of the half-tone mask for grey level N°154 in the 'calibration' layout

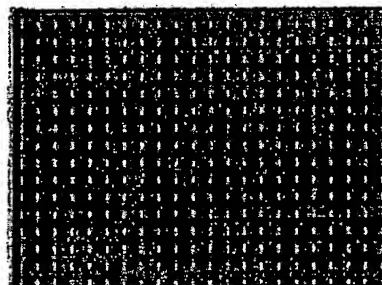


Figure 3 : Picture of the half-tone mask for grey level N°252 in the 'calibration' layout

On Figure 2 and Figure 3, the quartz looks grey and the chrome looks bright. For encoding grey level 252 in the mask, L-shaped clear apertures in the chrome layer are large, whereas they are quite small for encoding grey level 154. After the reduction induced by the lens, light passing through mask features of grey level 252 will not be attenuated much. Corresponding ablated structures will be deep. In the opposite, light passing through mask features of grey level 154 will be attenuated in a stronger manner. Ablation depth will be shallower.

### 3 PROCESS CHARACTERIZATION

The half-tone mask we made contains several DOE layouts and a specific layout for characterizing the ablation process. This latter layout (we called it 'calibration') is aimed at deriving the ablation depth curve as a function of the half-tones encoded in the mask, for each different substrate considered. It was designed as a portable grey map (PGM) file, which is a raster image format with grey level information recorded for each pixel. A PGM file can contain 256 grey levels (8 bits-per-pixel).

The 'calibration' PGM file is a 200x200 pixels image. It consists of an array of 64 identical geometrical features with a different grey level for each. The complete image therefore contains 64 grey levels. Each feature comprises 3 square patterns of identical shape (5x5 pixels) and grey level value. On top of each feature, the value of the grey level is indicated. The 64 grey levels of the layout are made of the successive values taken by the geometrical series starting at 0 (black) with 4 as an increment. The last grey level value is 254 (c.f. Figure 4). In the chrome-on-quartz half-tone reticle, each pixel corresponds to a 50  $\mu\text{m}$  square cell. The overall 'calibration' layout therefore covers 10 mm x 10 mm while a square pattern on it is a 250  $\mu\text{m}$  x 250  $\mu\text{m}$  square.

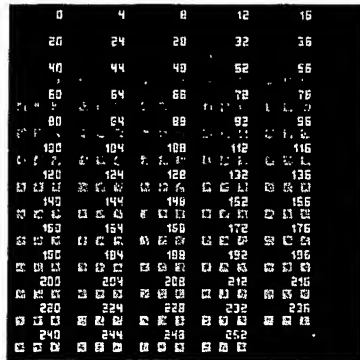


Figure 4 : 'Calibration' layout

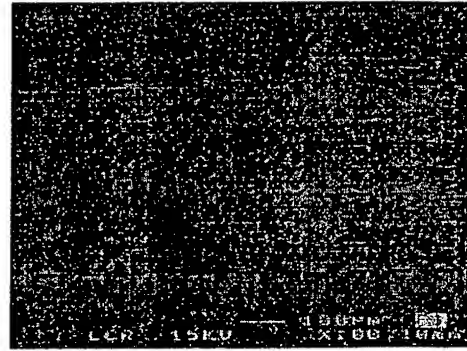


Figure 5 : SEM picture of the 'calibration' layout in a PC plate. Ablation was done at 0.4 J/cm<sup>2</sup> laser fluence with 32 pulses

Laser ablation through the 'calibration' layout was undertaken on three different substrates : 10 mm thick polycarbonate (PC) sheets, 1.5  $\mu$ m thick Shipley 1813 photo-resist spun on 4" glass wafers and 6.5  $\mu$ m thick benzocyclobutene (BCB) spun on 4" silicon wafers.

For each of these substrates, we repeated the half-tone ablation process several times with different laser fluences and numbers of laser pulses: 0.1, 0.2, 0.4, 0.6 or 0.8 J/cm<sup>2</sup> for the laser fluence, and, 1, 2, 4, 8, 16 or 32 laser pulses. Figure 5 is a SEM picture of the layout micromachined in a PC sheet by means of laser ablation through the halftone mask. The laser fluence was set to 0.4 J/cm<sup>2</sup> and the number of pulses was 32. Clearly visible are the ablation depths varying with the grey levels.

For each of the samples we made ablation depth measurements with a Dektak 8000 stylus profilometer. The results are presented for polycarbonate and benzocyclobutene in the following graphs (see Figure 6 and Figure 7). Each curve represents the ablation depths as a function of the grey levels encoded in the mask for a specific fluence and a specific number of pulses. In the legend of these graphs, F means fluence in mJ/cm<sup>2</sup> and N number of pulses of the laser.

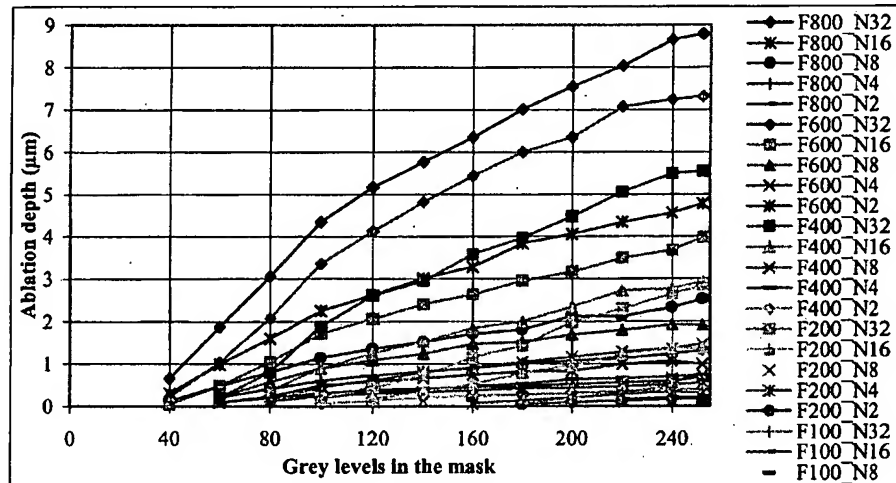


Figure 6 : Depth of the ablated structures in PC as a function of grey levels for different laser fluence and different number of laser pulses.



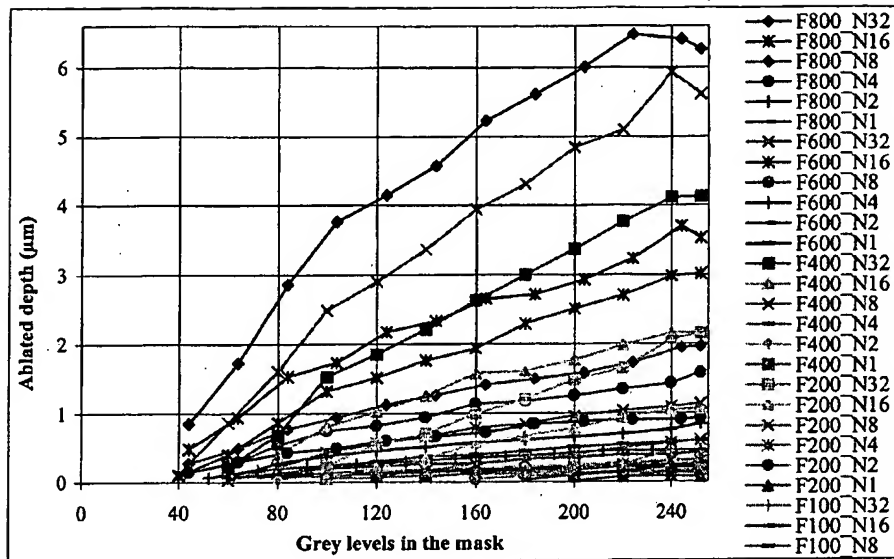


Figure 7 : Depth of the ablated structures in BCB as a function of grey levels for different laser fluence and different number of laser pulses.

On Figure 6 and Figure 7, one can see that the ablation depth responses of the material to the grey tones are not linear curves. However, the lower the fluence is, the more linear the corresponding ablation depth curve looks. SEM pictures of the ablated samples are shown in Figure 8, Figure 9, Figure 10 and Figure 11.

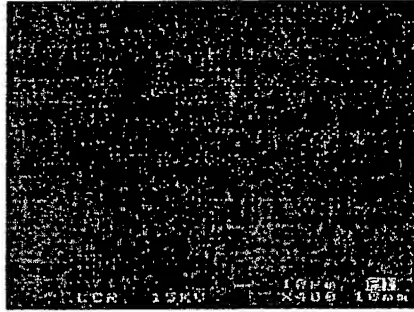


Figure 8 : Ablation on PC for gray level 200  
( $F = 0.4 \text{ J/cm}^2$ ,  $N = 32$ )

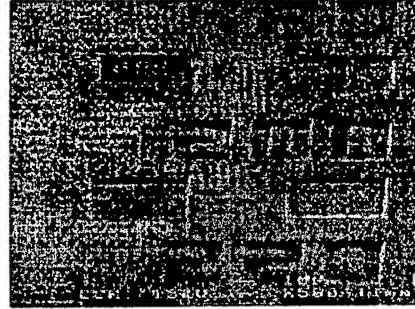


Figure 10 : Ablation on BCB for gray level 200  
( $F = 0.4 \text{ J/cm}^2$ ,  $N = 32$ )

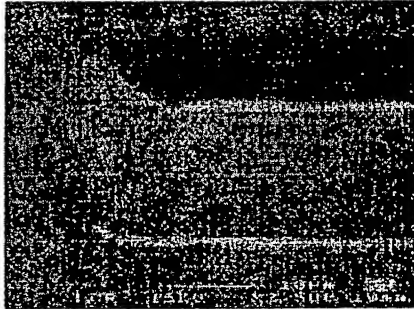


Figure 9 : Ablation on PC for gray level 200  
( $F = 0.4 \text{ J/cm}^2$ ,  $N = 32$ )

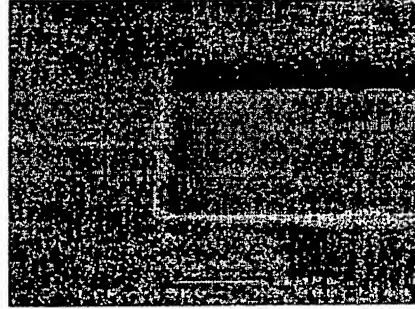


Figure 11 : Ablation on BCB for gray level 200  
( $F = 0.4 \text{ J/cm}^2$ ,  $N = 32$ )

In the case of polycarbonate, the ablated areas are very smooth and the surface roughness is very good. There is no thermally affected area around the ablated regions, except at high fluence ( $0.8 \text{ J/cm}^2$ ) for a high number of laser pulses (32 pulses). The sidewalls are not steep as can be seen on Figure 9.

BCB shows a stronger thermal effect around the ablated areas. Debris can be observed outside the ablated zones. Where the material has been ablated, there is less debris, but still significantly more than in the case of PC. The steepness of the sidewalls is much better than in the case of PC. In Figure 10 and Figure 11, middle of the ablated square, one can observe the track of the profilometer stylus' path. Such a mark is not observable on polycarbonate samples although ablation depths were also measured on them with the same profilometer and same parameters. In fact, this shows clearly that there is a thin layer of debris on top of the non-ablated BCB areas and that the stylus might have swept the particles present on its path. Particle redeposition is also observed on low fluence / low number of pulses samples. Particle redeposition might be reduced by strengthening the air blow at the surface of the sample during the ablation process.

## 4 DOE FABRICATION

### 4.1 DOE design

The DOEs present on the mask are simple DOEs specifically designed for process characterization. They consist of kinoforms and CGHs designed with software based on the Gerchberg-Saxton algorithm<sup>8</sup>. The Gerchberg-Saxton algorithm is an iterative Fourier transform algorithm based on scalar diffraction theory. It is aimed at designing pure phase elements which can reconstruct either in the near field (Fresnel elements) or in the far field (Fraunhofer elements). CGH phase distribution is encoded as a PGM grey level image file, in which a grey level simply represents a relief level. Up to 256 relief levels elements can therefore be designed.

All the DOEs we generated are transmissive elements calculated for a plane wave illumination at wavelength equal to 633 nm or 850 nm. They have 2, 4 or 8 relief levels with pixel sizes of 5 or 10  $\mu\text{m}$ . We made very small elements (51 x 51

pixels) and larger ones (512 x 512 pixels). Figure 12 is the image of the 4-level CGH, called "lamar\_cgh", which reconstructs the word LAMAR in the far field. Simulated reconstruction for a plane wave illumination at 633 nm is shown in Figure 13. The simulated diffraction efficiency is 78.3%. This element is quite small (128 x 128 pixels) and has pixel dimension of 10 µm. In Figure 12 (PGM file), the 4 phase levels are represented as 4 grey levels. The grey level values are 255 (white), 170, 85 and 0 (black). The same grey tones are encoded in the mask. By means of the ablation through the halftone mask, black pixels will not be ablated, whereas ablated structures will be the deepest at white pixels locations.

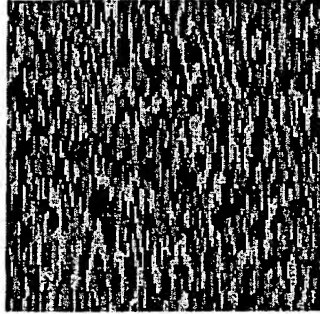


Figure 12 : Lamar\_cgh, 128x128 pixels, 4 relief levels, pixel size 10 µm

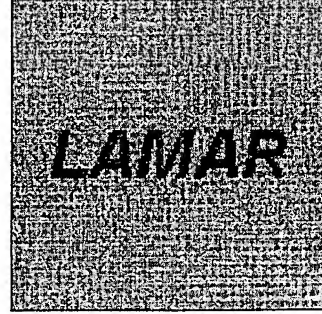


Figure 13 : Simulated reconstruction

In scalar diffraction theory, the height difference between two consecutive phase levels is given by :

$$h = \frac{\lambda}{N \times (n-1)} \quad (2)$$

where  $\lambda$  is the wavelength of the laser used to illuminate the DOE,  $N$  is the total number of phase levels of the DOE and  $n$  is the refractive index of the material. For example, for machining a 4-level element in polycarbonate (refractive index = 1.58), with a design wavelength of 633 nm, the height difference between 2 consecutive levels should be approximately 0.27 µm.

When encoding the CGH relief levels as a PGM image, the different relief levels calculated are linearly encoded in grey levels, with 0 (black) corresponding to the largest phase value (highest relief) and 255 (white) to the lowest (deepest structure). As a consequence, the relief levels of the DOEs will be correctly micromachined not only if the fluence and the number of pulse of the laser are correctly chosen but also if there exist a linear relation between ablation depths and grey levels encoded in the masks.

#### 4.2 DOE micromachining

From the 'calibration' layout analysis we know the ablation depths as a function of the various grey levels encoded in the mask for different laser fluences and different numbers of laser pulses. For manufacturing DOEs, we now have to select the laser fluence and the number of pulses that best fit the required relief levels of a specific DOE. In Figure 14 and Figure 15 the various ablation curves in polycarbonate are plotted which best match the depth range of 4- and 8-level CGHs.

In the legends of Figure 14 and Figure 15,  $F$  means fluence in  $\text{mJ}/\text{cm}^2$  and  $N$  number of pulses of the laser. The dotted curves represent the heights required for realizing a CGH according to its number of phase relief  $N_r$  and to its operating wavelength. The curve named DOE\_N4\_850 therefore indicates the heights required for a 4-phase element operating at 850 nm in PC.

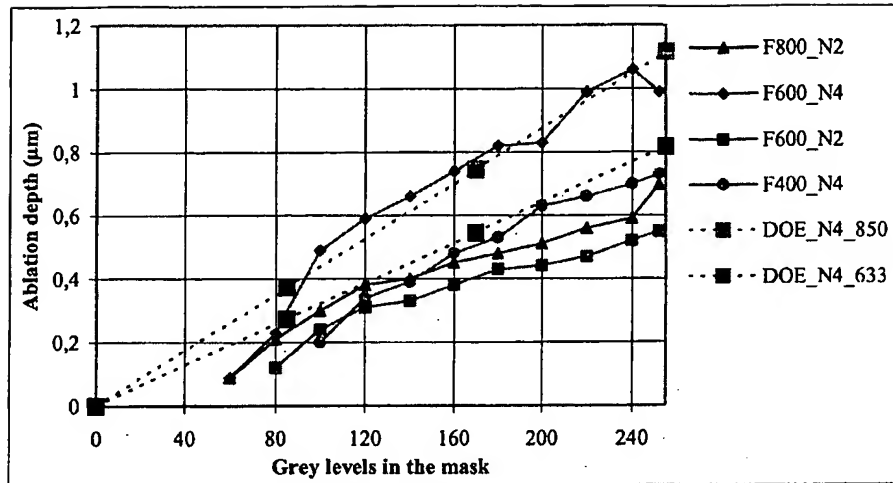


Figure 14 : Depth of the ablated structures in PC as a function of grey levels versus required relief levels for a 4 phase levels CGH in PC

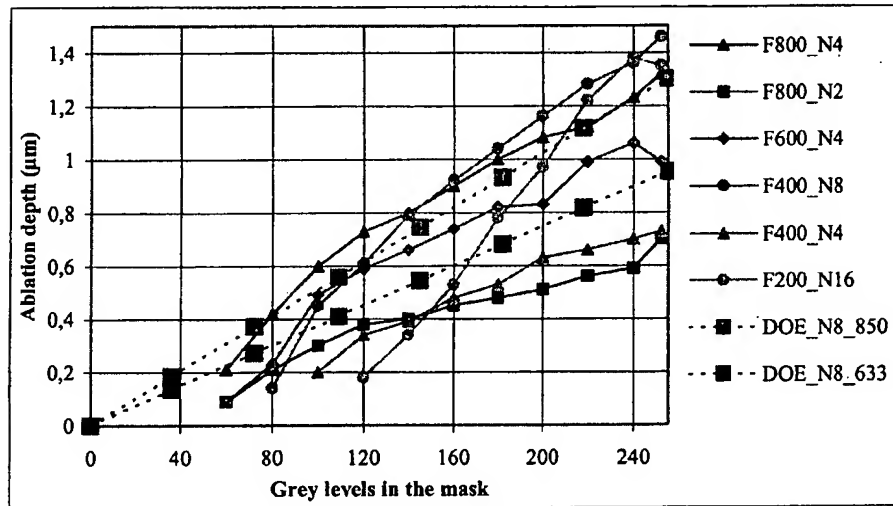


Figure 15 : Depth of the ablated structures in PC as a function of grey levels versus required relief levels for a 8 phase levels CGH in PC

As can be seen, no perfect matching occurs between the required heights and the ablation depths we measured. However, for manufacturing a 4 phase level element working at 633 nm in PC, several laser settings are close to what would be suitable : 4 lasers pulses at 0.4 J/cm<sup>2</sup>, 2 laser pulses at 0.8 J/cm<sup>2</sup>.

It is important to note here that the DOEs we show in this paper were processed before the ablation process was fully characterized. We therefore had to make assumptions for setting up the KrF laser. For machining 4-level elements operating at 633 nm, relief depths corresponding to grey levels 85, 170 and 255 should respectively be equal to 0.27, 0.54 and 0.81 μm. To do so, we made ablation trials with 3 pulses at 0.8 J/cm<sup>2</sup>, 4 pulses at 0.6 J/cm<sup>2</sup>, 5 pulses at 0.4 J/cm<sup>2</sup> and 10 pulses at 0.2 J/cm<sup>2</sup>.

The resulting ablation depths obtained are too deep compared to what we were seeking. For 3 pulses at  $0.8 \text{ J/cm}^2$ , 4 pulses at  $0.6 \text{ J/cm}^2$ , 5 pulses at  $0.4 \text{ J/cm}^2$  and 10 pulses at  $0.2 \text{ J/cm}^2$ , the maximum ablation depths are respectively equal to  $1.09 \text{ }\mu\text{m}$ ,  $1.14 \text{ }\mu\text{m}$ ,  $1.12 \text{ }\mu\text{m}$  and  $1.03 \text{ }\mu\text{m}$ . Such errors in relief levels heights will lead to important non-diffracted light (zero order of diffraction) at the reconstruction plane.

Figure 16 and Figure 17 are SEM pictures of the 4 phase lamar\_cgh made in PC by KrF laser ablation through the halftone mask. Laser fluence was set to  $0.4 \text{ J/cm}^2$  for 5 pulses.

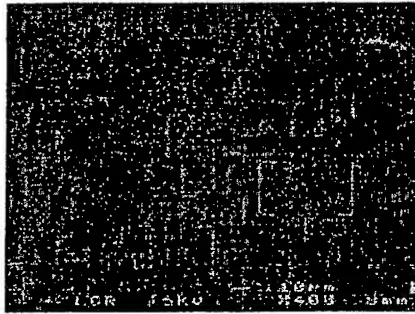


Figure 16 : SEM picture of the lamar\_cgh in PC for  $F = 0.4 \text{ J/cm}^2$  and  $N=5$  pulses



Figure 17 : SEM picture of the lamar\_cgh in PC for  $F = 0.4 \text{ J/cm}^2$  and  $N=5$  pulses

Roughness measurement of the DOEs relief levels in PC gave typical  $R_a$  of approximately  $30 \text{ nm}$ , which is pretty good.

In the opposite, sidewalls angles of the ablated PC structures are very low. Besides, these angles also vary according to the ablation depths : the shallower the ablated structure, the lower the sidewall. In the case of machining the lamar\_cgh with 5 pulses at  $0.4 \text{ J/cm}^2$ , we measured sidewall angles varying from  $6$  to  $10^\circ$ . In the case of DOEs made in BCB, the ablated structures have much better steepnesses. AFM measurements showed sidewall angles in BCB up to  $57^\circ$ .

Another difficulty in machining the DOEs rises from the non-linearity of the ablation depth responses to the grey level encoded in the mask. In the case of a 4 phase levels CGH, the relief height between grey level 0 and 85 should be equal to the relief height between grey level 170 and grey level 255. Due to the non-linearity of the ablation response, these two step heights will be different in the material. Therefore, the corresponding phase steps will not be equal anymore and as a consequence, errors will occur in the optical reconstruction.

Such differences in the ablation depth of two identical phase steps are clearly visible in the CGHs made in PC at high fluences (trials with 3 laser pulses at  $0.8 \text{ J/cm}^2$  and 4 pulses at  $0.6 \text{ J/cm}^2$ ). Indeed, samples ablated at high fluences showed stronger non-linearity in their responses. For lower fluence experiments (trials with 10 laser pulses at  $0.2 \text{ J/cm}^2$  and 5 pulses at  $0.4 \text{ J/cm}^2$ ), since the ablation curves are closer to straight lines, height differences corresponding to identical phase step do not vary much.

#### 4.3 Optical Measurements

We made optical characterizations of the DOE realised in PC. As noted previously, because the fabricated elements don't have the correct depths and sidewall angles, important errors occur in the optical reconstruction.

Most importantly, due to the depth errors, a significant amount of non-diffracted light (0 order of diffraction) is present in the reconstruction plane. Furthermore, because the sidewalls are not steep there is also lot of energy located in high diffraction orders. Noise is also evident surrounding the first order of diffraction.

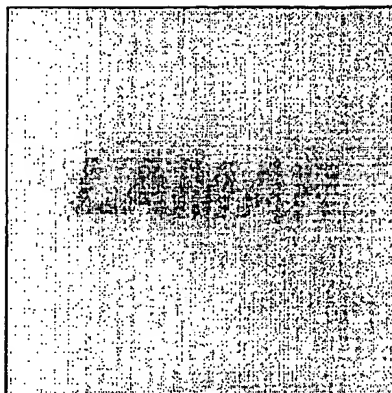


Figure 18 : Reconstruction in the far field of the lamar\_cgh. The DOE was realized through the halftone mask with 5 shots at  $0.4 \text{ J/cm}^2$

Figure 18 is the far field reconstruction (first order of diffraction) of the light diffracted by a lamar\_cgh DOE realized with 5 laser shots at  $0.4 \text{ J/cm}^2$ . The laser used was a HeNe laser at  $632.8 \text{ nm}$  wavelength. The figure of diffraction was taken by a Cohu 6700 CCD camera.

## 5 CONCLUSION

Fabrication of diffractive optical elements by means of excimer laser ablation through a half-tone mask has been presented in this paper. Half-tone masks are binary masks, in which the critical feature size is smaller than the resolution limit of the optical exposure system. Arrays of such small features act in fact as light attenuators and therefore make possible modulation of the transmission of the mask. At the substrate, the incident fluence varies correspondingly, which enables multi-level ablation.

Several DOEs were realized in polycarbonate by this technology. However since the process was not fully characterized when the DOEs were processed, we did not reach the proper heights in the material. Furthermore, the ablated structures in PC have very low sidewall angles, which is a major drawback for DOE fabrication. Consequently, diffraction efficiencies of the samples we made are quite low.

To improve our results in the field of DOE manufacturing, many tasks are scheduled. Firstly, samples will be machined with optimised laser set up. Secondly, the way to encode grey levels in the mask will be slightly changed in order to take into account the non-linearity of the material response. Finally other materials than PC will also be investigated.

## ACKNOWLEDGMENTS

The authors would like to thank Exitech staff for their assistance in performing the experiments. This work was supported by the Bright Euram European project LAMAR (BE97-5123).

## REFERENCES

1. M. T. Gale, M. Rossi, J. Pedersen, H. Schütz, "Fabrication of continuous-relief micro-optical elements by direct writing in photoresists", *Optical Engineering*, **33**, pp. 3556-3566, 1994.
2. W. Däschner, M. Larsson, S. H. Lee, "Fabrication of monolithic diffractive optical elements by use of e-beam direct write on an analog resist and single chemically assisted ion-beam-etching step", *Applied Optics*, **34**, pp. 2534-2539, 1995.
3. G. P. Behrmann, M. T. Duignan, "Excimer laser micromachining for rapid fabrication of diffractive optical elements", *Applied Optics*, **36**, pp. 4666-4674, 1997.
4. X. Wang, J. R. Leger, R. H. Rediker, "Rapid fabrication of diffractive optical elements by use of image-based excimer laser ablation", *Applied Optics*, **36**, pp. 4660-4665, 1997.

5. Y. Oppliger, P. Sixt, J. M. Stauffer, J. M. Mayor, P. Regnault and G. Voirin, "One-step 3D shaping using a gray-tone mask for optical and microelectronic applications", *Microelectronic Engineering*, **23**, pp. 449-454, 1994.
6. J. Su, J. Du, J. Yao, F. Gao, Y. Guo, Z. Cui, "A new method to design half-tone mask for the fabrication of continuous micro relief structure", *Proc. SPIE*, 3680, pp. 879-886, 1999.
7. W. Henke, W. Hoppe, H. J. Quenzer, P. S. Fischbach, B. Wagner, "Simulation and process design of gray-tone lithography for the fabrication of arbitrarily shaped surfaces", *J. Appl. Phys.*, **33**, pp. 6809-6815, 1994.
8. "HEBS-glass photomask blanks", Product information 94-88, Canyon Materials Inc, 6665 Nancy Ridge Drive, San Diego, CA, 92121.
9. S. J. Mihailov, F. Bilodeau, K. O. Hill, D. C. Johnson, J. Albert, A. S. Holmes, "Apodization technique for fiber grating fabrication with a halftone transmission amplitude mask", *Applied Optics*, **39**, pp. 3670-3677, 2000.
10. R. W. Gerchberg, W. O. Saxton, "A practical algorithm for the determination of phase from image and diffraction plane pictures", *Optik*, **35**, pp. 237-246, 1972.

# Industrial Research Institute Swinburne



## ➤ About IRIS

### ➤ Research Activities

- Bio Technology
- Intelligent Manufacturing Systems
- Laser Technology
- Micro Technology
- Microwave Technology
- Robotics & Non Contact Inspection

### ➤ Degree Programs

### ➤ Technology Diffusion

### ➤ Industry Collaboration

### ➤ Strategic Links

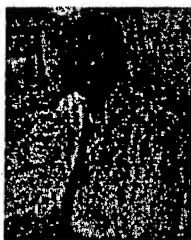
### ➤ IRIS Operational Chart

### ➤ Nanotechnology

### ➤ Contact Information

### ➤ Faculty of Engineering & Industrial Sciences

## Micro Technology



### Research Leader:

**Prof. Erol Harvey**  
Email: [eharvey@swin.edu.au](mailto:eharvey@swin.edu.au)  
PhD: Monash University, 1989  
B.Sc.: Monash University, 1985

### Research Activities:

Excimer Laser Micromachining Technology  
Microsensors  
Micro Optics  
UV Material Modification  
MEMS, MST, MOEMS and Microengineering

A/Prof Erol Harvey received his Ph.D in Physics from Monash University in 1988. He moved to the UK where he became Operations Manager of the SPRITE laser facility of the SERC Rutherford Appleton Laboratory near Oxford. In 1991 he moved to Exitech Limited, a spin-out company from the Rutherford Laser Facility, where he was Principal Development Engineer and Head of System Design and Fabrication of the Advanced Excimer Laser Micromachining systems. In this role he has been the project co-ordinator for Workstation Design and fabrication for customers throughout Japan, Europe, Asia and the Far East, and has worked closely with customers around the world developing applications

- Manufacturing Technologies
- CRC for Manufacturing Technologies

### Typical Publication and Patents:

1. E C Harvey, T R Mackin, R E Scholten "Micro optical structures for atom lithography" SPIE Vol 3892, 28 Oct 1999, pp
2. M Ghantasala, E Harvey and D Sood "Excimer laser micromachining of structures using SU-8", SPIE Vol 3874, 20 Sep 1999, pp85-91
3. N.H.Rizvi, E.C. Harvey, P.T. Rumsby, J.P.H. Burt, M.S. Talary, J.A. Tame and R. Pethig, "An Excimer Laser Micromachining System for the production of Bioparticle Electromanipulation Devices" SPIE Vol 3224, 29 Sept 1997, pp266 - 272
4. P.T. Rumsby, N.H. Rizvi, E.C. Harvey and D. Thomas "Excimer laser patterning of thick and thin films for high-density packaging", In "Microelectronic Packaging and Laser Processing" SPIE Vol 3184, 25 June 1997, pp 176 - 185
5. E.C. Harvey and P.T. Rumsby "Fabrication techniques and their application to produce novel micromachined structures and devices using excimer laser projection" in "Micromachining and microfabrication process technology III" SPIE Vol 3223, 25 June 1997, pp26 - 33
6. P.T. Rumsby, E.C. Harvey and D.W. Thomas "Laser Microprojection for Micromechanical Device Fabrication" SPIE

Contact Info:  
Industrial Rese  
Swinburne  
T +61 3 9214 8  
F +61 3 9214 5  
[iris@swin.edu](mailto:iris@swin.edu)  
[www.swinburn](http://www.swinburn)



- [ 7. Vol 2921, 4 Dec 1996, pp684 – 692  
Erol C Harvey, Phil T Rumsby, Malcolm C Gower and Jason L Remnant "Microstructuring by Excimer Laser" SPIE Vol 2639, 23 Oct 1995, pp266 – 276 ]
8. Erol C Harvey, Phil T Rumsby and Malcolm C Gower "Excimer laser projector for materials processing applications", Proc. Laser Advanced Materials Processing LAMP92, High Temperature Soc. Japan, 1992, pp1047-1052
9. E C Harvey, C J Hooker, M H Key, A K Kidd, M D Lister, M J Shaw and W T Leyland "Picosecond gain and saturation measurements in a KrF laser amplifier depumped by amplified spontaneous emission", J.Appl.Phys, 70(10), 1991, pp5238-5245
10. J M D Lister, M J Shaw, C J Hooker and E C Harvey "Uniform target illumination by spatial incoherence in a multiplexed KrF laser system", Optics.Comm,84(1,2), 1991, pp55-60
11. I N Ross, M J Shaw, C J Hooker, M H Key, E C Harvey, J M D Lister, J E Andrew, G J Hurst and P A Rogers "A high performance excimer pumped Raman Laser" Opt.Comm, 78(3,4), 1990, pp263-270
12. E C Harvey and M J Shaw "A simple kinetic model for electron beam-pumped KrF lasers", Laser&Part. Beams, Feb2 1990
13. E C Harvey, P T Rumsby, T Wheelwright, Coinventors Patent Application "Laser engraving of integro printing plates for bank notes and security printing" (Europe, 20 Feb 1996)
14. R C Tobin, E C Harvey, A K Anders Coinventors Patent "Room temperature metal vapour laser", USA 4771435, Sept 13, 1998
15. R C Tobin, E C Harvey, A K Anders, Coinventors Patent "Room temperature metal vapour laser" Australia 65352/86, Europe 87100909.8

#### Typical Research Projects:

Patterning Thin Films for Sensors  
UV Modification of Polymers for Enhanced Bio-compatibility  
Novel Structures Using Rotating Masks  
SU-8 Ablation for Rapid High Aspect Ratio 3D Microfabrication  
Femtosecond Laser Ablation  
Dynamic Measurements of Microsystems  
Micro Optics for Atom Lithography  
New Machining Strategies for Glass  
New Machining Strategies Using Excimer Mask and Workpiece Draggings.

# Microstructuring by Excimer Laser

Erol C Harvey, Phil T Rumsby, Malcolm C Gower, Jason L Remnant

Exitech Limited, Hanborough Park  
Long Hanborough, Oxford OX8 8LH

## ABSTRACT

Excimer laser ablation provides the micromachining engineer with a unique tool for patterning, cutting and structuring a wide variety of materials, including ceramics, glasses and polymers. The short pulse (20ns) ultra violet laser beam is used for non-thermal ablative material removal producing structures with a depth resolution of the order of 0.1 $\mu$ m and spatial resolutions of the order of 1 $\mu$ m or better. Careful control of laser dose (usually done using CNC systems) enables multi-level machining to be performed producing 3 dimensional microstructures which maybe used directly, or as mould tools for laser-LIGA replication. This talk aims to illustrate both the possibilities, and limitations, of micromachining by excimer laser ablation, and will highlight some practical examples of structures and devices manufactured using this tool, many of which are currently in or near commercial production.

**Keywords:** excimer laser, microengineering, Laser-LIGA, 3D microstructures.

## 1. INTRODUCTION

Excimer lasers are pulsed gas lasers which produce ultraviolet radiation in the range of 351nm to 193nm depending upon the composition of the gas mix used. For the purposes of direct ablative micromachining the most useful wavelengths are 248nm (Krypton Fluoride) and 193nm (Argon Fluoride). The laser pulses are short (typically of the order of 20ns) and have a pulse energy at the laser exit of between 10mJ and 1000mJ. Industrially useful machines produce pulse energies of around 500mJ at repetition rates of up to 200 Hz, thus giving average powers of the order of 100W.

Exit beams from the laser aperture are rectangular with aspect ratios of about 2:1 and areas of  $\sim 2\text{cm}^2$  and usually have a gaussian-like intensity profile across the narrower direction and a supergaussian profile across the other. Typically 75% of the total energy of the pulse shows a spatial intensity deviation from the mean of  $>\pm 35\%$ . For most applications the large beam inhomogeneities are unsatisfactory since beam intensity variations usually become replicated into the processed material. To overcome this limitation various optical beam homogenization methods are employed in the beam delivery train of processing systems. Homogenization is performed by breaking up the laser beam into a multiplicity of components and overlapping each part at a predetermined position thus averaging out inhomogeneities. Homogenizers use components such as diffuser plates, microlens arrays (fly's eye homogenizers), kaleidoscopes, fibres,

mirrors or prisms to perform this function and can achieve intensity profiles with RMS deviations of less than  $\pm 5\%$  and overall throughput efficiencies of up to 70%.<sup>1</sup>

The energy density, or fluence, produced at the exit of the laser is about  $250 \text{ mJ/cm}^2$ . This is generally too low to be useful for machining applications since polymers, for example, typically require  $800 - 1000 \text{ mJ/cm}^2$  for efficient machining. Ceramics and glasses require fluences an order of magnitude higher. Imaging or projection lenses are used to concentrate the beam onto the workpiece and achieve useable fluences. The role of the projection lens is to transfer the plane of uniformity, i.e. the position in the optical train at which the homogenizer overlaps the beam components, to the workpiece with suitable demagnification in order to achieve the working fluence.

A mask is placed at the plane of uniformity of the homogenizer so that the projection lens images the mask onto the workpiece. The mask may be a simple aperture, square or circular, or may be a more complex structure enabling complex shapes to be ablated into the workpiece in a single step. The mask may be formed from a wide variety of materials. Copper, brass or stainless steel sheet may be chemically milled or Nd:YAG laser cut to produce the mask, or simple bench-top photolithography may be used to produce a chrome-on-quartz mask of higher resolution. The tolerances with which the mask must be made is determined by multiplying the intended tolerances at the workpiece by the magnification factor of the projection lens. The fluence at the workpiece is equal to the square of the projection lens magnification multiplied by the fluence at the mask plane. A chrome-on-quartz mask is only appropriate if fluences at the mask plane are under  $100 \text{ mJ/cm}^2$ . For systems requiring higher mask-plane fluences or using lower magnification factors, a more expensive patterned dielectric reflective mask may be used.

## **2. EXCIMER LASER PHOTOABLATION**

Most materials absorb strongly in the ultraviolet so that the laser pulse is typically absorbed within less than  $1 \mu\text{m}$  of the surface. Photons with a wavelength of  $248 \text{ nm}$  (KrF radiation) have an energy of about  $5 \text{ eV}$  which is sufficient to cause photodissociation, particularly of organic polymers for which the process is most efficient. The rapid breaking of chemical bonds causes a sudden pressure increase within the absorption region and forces material to be ejected in a mini-explosion. Since typical excimer laser pulse durations are around  $20 \text{ ns}$  the interaction with the material occurs very rapidly. This key element to photoablation means that the time for thermal transfer through the workpiece is short and thermal damage to side walls and surrounding structures is minimised. Excimer laser micromachining is often classified as a non-thermal process, although there are instances in which highly localised thermal effects can be produced by the laser. (Commercial applications of such thermal processes include annealing of amorphous silicon and stainless steel hardening.)

The rate at which material may be machined by an excimer laser is a function of the fluence incident upon the surface. Figure 1 shows a typical ablation rate curve for polyimide as a function of fluence for three

excimer laser wavelengths. The ablation rate for 248nm radiation at an incident fluence of 800 mJ/cm<sup>2</sup> is about 0.25µm per pulse. In order to machine to a depth of 1.0µm four pulses would be required. The ability to control the depth of machining simply by counting the number of incident laser pulses is an important aspect of the use of excimer lasers for micromachining, and a task readily handled by the laser processing system controller.

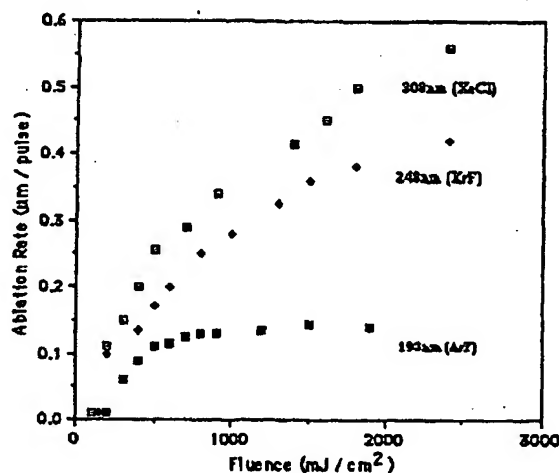


Figure 1. Ablation etch rate curve for Polyimide

### 3. CONTROL OF ABLATED WALL ANGLE

#### 3.1 Influence of fluence and numerical aperture

The wall angle of the ablated site is dependent upon many factors, but most importantly upon the incident fluence and the numerical aperture of the projection system. Figure 2 shows the cross section of square holes ablated through 100µm thick polyethyleneterephthalate (PET) sheet using 248nm (KrF) radiation and a 0.2 NA objective. The image of the aperture is 50µm x 50µm at the surface of the sheet which is at the top of the figure. The sample was held stationary during ablation and not moved towards the objective during machining even though the distance between the ablation site and the objective increases as material is removed.

At small fluences the hole tapers inwards (positive taper) due to diffraction effects at the entrance. At higher fluences the taper angle reduces until the walls undercut the surface (negative taper). Since the NA of the objective is high some of the light rays forming the image of the aperture are incident upon the surface at high angles. As machining proceeds these rays can ablate the material provided they do not suffer excess attenuation due to diffraction at the ablation site entrance i.e. provided the fluence is high

enough. The path of these rays through the material causes undercutting. Figure 3 shows the dependence of wall taper upon incident fluence for PET and Upilex (polyimide) machined at 248nm.



Figure 2. 50µm square holes ablated through 100µm thick PET using 248nm radiation and 0.2NA objective. Laser is incident at the top with fluences of (i) 0.87/cm<sup>2</sup> (ii) 0.47/cm<sup>2</sup> (iii) 0.27/cm<sup>2</sup> (iv) 0.157/cm<sup>2</sup> (v) 0.157/cm<sup>2</sup> and (vi) 0.10J/cm<sup>2</sup>

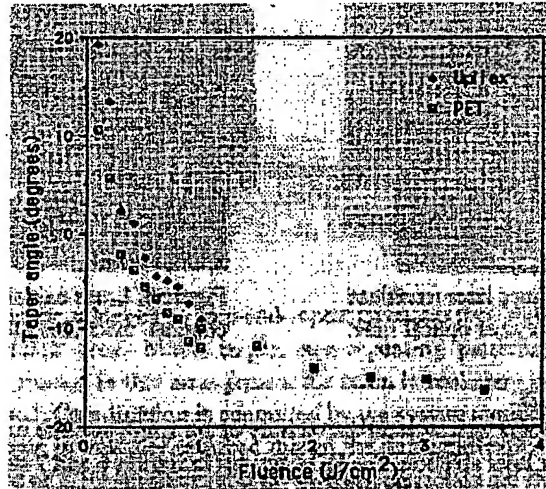


Figure 3. Dependence of ablated wall angle upon incident fluence for PET sheet machined using 248nm, 10Hz repetition rate, 0.3NA objective

Practical examples of holes machined with controlled taper are shown in figures 4 and 5. Figure 4 shows rectangular holes ablated through a 175µm diameter polymer optical fibre to produce a blood gas monitoring catheter. The rectangular holes have an input size (laser incident side) of 50µm x 90µm ±10µm and a laser exit size of 25µm x 50µm ±10µm. The NA of the projection optics used to form the rectangular aperture is different for the two orthogonal axes and hence the taper angle of the hole differs for each axis. The tolerance on the volume of the rectangular holes is important for the calibration of the sensors.

Figure 5. shows the rear, or laser exit side of a bifurcating channel machined into polyimide. The high NA projection lens formed the image of a rectangular aperture on the upper surface of the polymer sheet by combining the two beam paths from the homogenizer illuminating the aperture at the mask plane. By working at high fluence the setup machined a rectangular aperture on the surface of the polymer and broke through the rear surface of the polymer as two undercut rectangular channels. The shape of the hole is determined by the shape of the aperture at the mask plane, hence a wide variety of differently shaped multiple channel structures may be machined. The number of channels may be increased by *increasing* the number of beam *components illuminating* the mask. For applications such as these great care must be taken to make the correct choice of the coherence factor, i.e. to match the NA of the beam splitting homogenizer to the NA of the final projection objective without affecting the intended resolution at the workpiece.

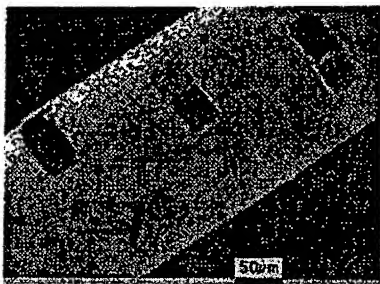


Figure 4. Rectangular apertures laser machined through 175µm diameter polymer optical fibre.

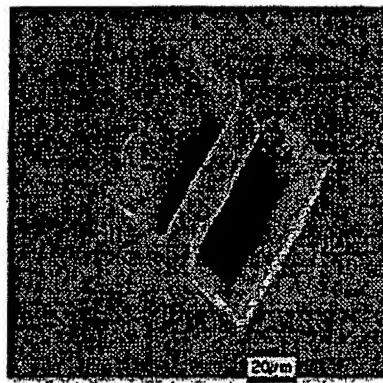


Figure 5. Laser exit side of bifurcated channel machined into polyimide sheet.

### 3.2 Assist gases and vapours

The action of gases or vapours which are in the vicinity of the irradiated site may also influence the wall angle produced by excimer laser ablation. The SEM images in figures 6 and 7 show this for direct ablation of silicon using 193nm (ArF) at 8.0 J/cm<sup>2</sup>.

Silicon does not easily ablate under direct laser illumination. The sample shown in figure 6 shows severe thermal damage to the wall edges so that the wall taper angle is dominated by melting and the bottom of the cut is rounded by melt flow. The sample shown in figure 7 was ablated in the presence of a fine mist of water vapour delivered by a precisely controlled nozzle. Although there is some evidence of "splatter" at the edges of the cut most of the thermal damage has been eliminated. It should be noted that the optical setup in this experiment was not optimized for resolution so that the edge quality is now limited by the optical resolution rather than melting. Chlorine has also been used as an assist gas, in this case for machining copper and stainless steel.

## 4.3D MICROMACHINING TECHNIQUES

### 4.1 Mask projection

The simplest method for excimer laser machining is to use a mask which contains the complete 2D structure of the shape to be cut. Typically the maximum practical area of the beam at the mask plane is about  $1\text{cm}^2$ . Larger mask illumination areas require complex and expensive projection optics in order to attain the ablation fluences required at the workpiece (photolithographic processes require much lower fluences and are therefore not applicable to this discussion).



Figure 6. Silicon machined by direct laser irradiation showing severe thermal damage

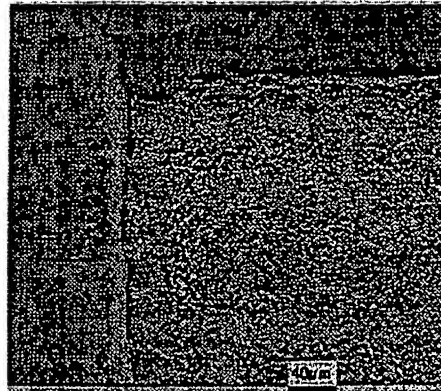


Figure 7. Silicon machined as in figure 6 with the use of vapour assist.

Patterning large areas may be achieved by step-and-repeat processes providing the repeating shape can be contained within the mask area. Much larger, non-repeating patterns may be machined using synchronously scanning masks. In this arrangement the beam is stationary and the workpiece and mask are synchronously scanned. Coordination is controlled by the system motion controller which also takes into account the difference in velocity required due to the demagnification and image reversal of the projection lens. Examples of 2.5D structures ablated by mask projection are shown in figures 8 - 11.

The mask used to machine the pattern shown in figure 9 was prepared using a laser printer and transparency film to prepare a negative which was transferred by contact exposure into the resist on a HOYA chrome-on-quartz blank. After a simple bench-top developing and etching process the resulting mask was placed into an Exitech Series 7000 Excimer Laser machining system and projected onto the workpiece using a 5x magnification refracting objective. The aliased edge of the laser printed pattern has been clearly resolved by the ablation process.

A machining system which is able to synchronously move the masks may also be used to index different masks producing the type of multi-level structures shown in figure 10.

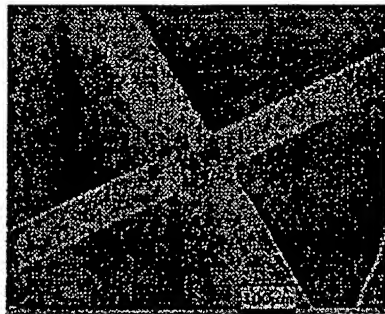


Figure 8. Cross ablated into PI using 248nm.

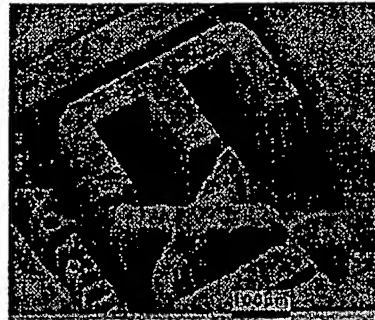


Figure 9. Pattern machined into Polycarbonate.

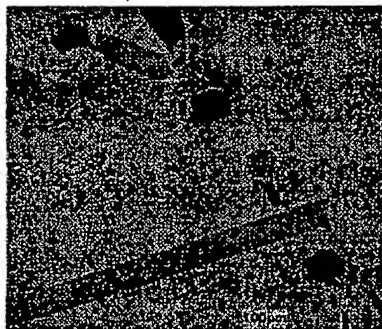


Figure 10. Two scanning masks were used to machine this structure, one for the holes and one for the reservoir.

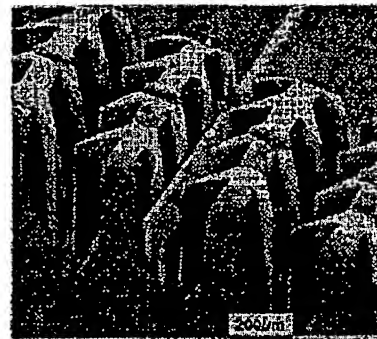


Figure 11. A fibre clamp machined into polymer using a step-and-repeat mask.

The ablation resolution is usually limited to about  $1\mu\text{m}$  when using projection lenses with reasonably large numerical aperture. The image resolution achievable with a lens can be increased by a factor of two compared to projection of a conventional chrome-on-quartz transmission mask by using a phase shifting mask<sup>2</sup>. Excimer laser micromachining of submicron structures using phase shifting mask projection was fast demonstrated in the production of Bragg gratings in optical fibres<sup>3</sup>. A 0.3NA lens and a single pulse from a broadband 248nm (KrF) laser was used to write a  $0.25\mu\text{m}$  lines and spaces grating 3mm long on the fibre that gave a peak reflectivity of 85% for a Bragg wavelength of  $1.53\mu\text{m}$  propagating down its core (figure 12).

Gratings on fibre optics such as that shown in figure 13 have applications as sensors (temperature, pressure and strain) and also as dispersion compensators in high bandwidth telecommunications networks.



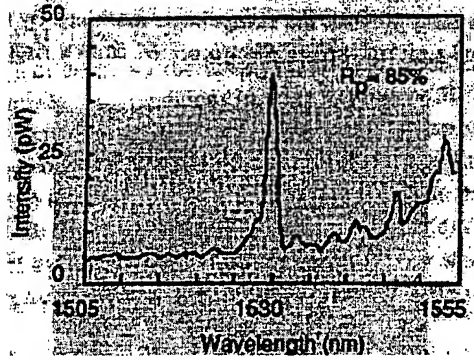


Figure 12. First order Bragg reflection spectrum from the fibre Bragg grating (FBG).

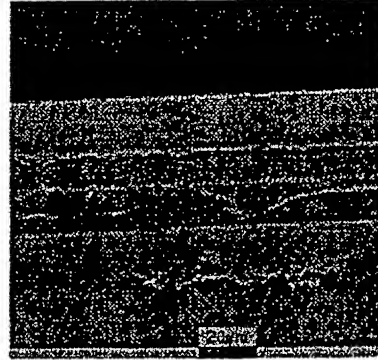


Figure 13. Grating written with a single KrF laser pulse into a Germanium doped optical fibre.

#### 4.2 Beam overlap

Each time the laser fires a fixed volume of material is removed. 3D structures may be machined by coordinating the motion of the workpiece, the mask, and the firing of the laser whilst keeping the beam stationary. A staircase structure may be machined by moving the workpiece in a step-wise fashion and using a fixed number of laser pulses per step. If the workpiece is moved at a fixed velocity while the laser fires at a constant repetition rate the resulting structure will be a ramp. The ramp angle may be varied by changing either the sample velocity or the laser repetition rate.

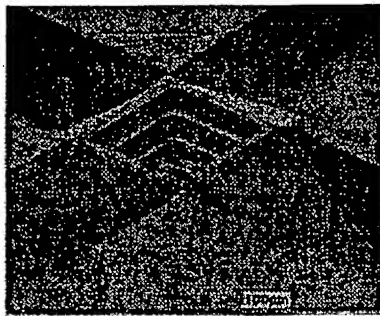


Figure 14. A pyramid and step structure ablated into PMMA using 193nm.

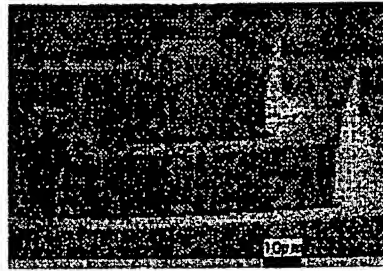


Figure 15. SEM of nickel replica electroformed from the structure shown in Fig. 14.

Figure 14 shows a structure ablated into PMMA using 193nm and a combination of each of these processes. The internal steps were machined using a computer controlled aperture which was partially closed between each burst of laser shots. Total machining time for this structure was 16 seconds.

Electroforming and injection moulding may be used to mass produce the components machined by the excimer laser<sup>4</sup>. Figure 15 is an SEM showing detail of a nickel replica electroformed from a similar structure to that shown in figure 14.

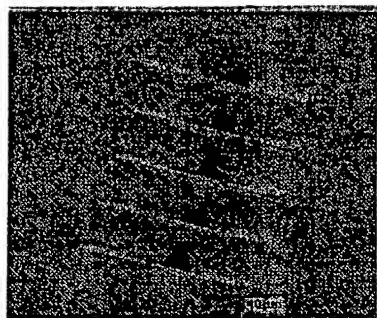


Figure 16. The inward curving faces of a fluid flow structure.



Figure 17. Upward curving structures machined by synchronized motion and laser firing.

Moving the workpiece through a carefully designed path also produces 3D structures. The concave array shown in figure 16 was machined using a mask with 5 circular apertures. The workpiece moved through a Lissajous path while the laser fired at a fixed incremental path distance producing walls with different curvatures in the orthogonal directions. The co-ordination and synchronized laser triggering was controlled by the Series 7000 system controller. If the sample accelerates during laser firing convex structures may be ablated, as shown in figure 17. Sophisticated CAD/CAM programming techniques have been used to demonstrate this type of machining by ablating a leather texture into an epoxy block<sup>5</sup>. After measuring a real leather sample a computer algorithm was used to break up the required shape into a matrix of square ablation sites at discrete machining depths or levels, and to write an optimum tool path. A computer driven aperture unit and position synchronized laser firing was used to ablate the required shape.

Multi-level structures may be ablated using masks which have more complex shapes. A mask with a "T" shaped aperture will ablate a 2-level structure with a "T" section if the workpiece is moved at a continuous speed while the laser fires at a fixed repetition rate. The leading and trailing ends of the "T" channel cut in this way would be ramps. "delta" apertures will give "V" channels, and "V" channels machined in two orthogonal directions will produce upstanding pyramids. This method of mask-dragging has been used to produce a microlens array using an appropriate curved aperture and machining in two or more crossed directions<sup>6</sup>.

Workpieces need not be planar, as shown by the catheter in figure 4. It is possible to construct an excimer laser micromachining lathe capable of micromachining cylindrical objects, such as fibres, by arranging the part to rotate axially while using the laser optics to project a mask or aperture radially or tangentially onto the workpiece. Turning, paring, side drilling and notching are all possible using such an arrangement.

### 4.3 Half tone mask

All of the above machining methods produce 2.5D structures, or require careful optimization of tool path and ablation conditions in order to produce 3D structures. An alternative method for producing complex structures is to use a mask with a variable transmission. Since high power uv beam attenuation methods cannot easily be used to manufacture a complex mask, an alternative approach is to make a binary mask, such as chrome-on-quartz, and use half-tone methods for producing variable transmission. A half-tone mask forms an image by varying the size of dots, each of which are too small to be resolved individually, but together produce an image with various shades. The images printed in this SPIE manuscript use this type of printing in order to reproduce the figures in this paper.

The pattern generated for a test half-tone mask is shown schematically in figure 18. Pairs of shaded blocks contain an area of fixed density separated from an area with varying density by a "ruler" made up of opaque squares. A black area in the figure represents an area of chrome on the mask, and hence an opaque area to the laser beam. In each pair one of the varying areas changes continuously, and the other in a step fashion.

The mask was made using an electron-beam writer to first prepare a chrome master. The master was then used as a photolithographic mask in a 10:1 scanner, exposing the resist on top of a chrome-on-quartz blank. After development the final mask was used in a Macro 5x demagnification Series 7000 excimer laser ablation system. The final chrome-on-quartz mask was made up of square apertures on a fixed  $5\mu\text{m}$  pitch. The squares varied in size from  $1\mu\text{m} \times 1\mu\text{m}$  (minimum transmission) to  $4\mu\text{m} \times 4\mu\text{m}$  (maximum transmission). The excimer laser imaging lens had a resolution of  $5\mu\text{m}$  at the workpiece.

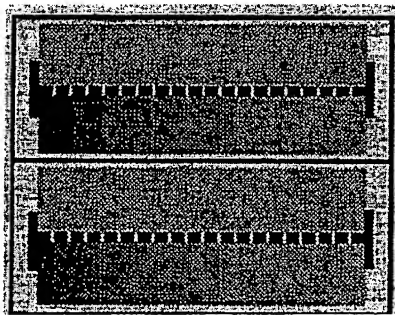


Figure 18. Schematic of one pair of patterns in a test chrome-on-quartz half-tone mask.

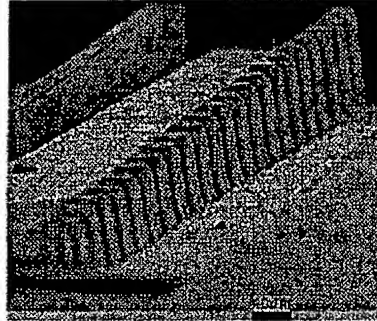


Figure 19. SEM of Polycarbonate machined through a half tone mask.

Polycarbonate sheet was ablated using 248nm, and afterwards measured to determine the profile of the resultant structure (figure 19). The unablated polycarbonate sheet was smooth and flat with a typical Ra value of 11nm. This value was largely dominated by dust on the surface. The upper end of the ablated ramp had a coarse texture with an Ra of 55nm. This is typical of ablation at low fluences where the

ablation process is very close to threshold<sup>7</sup>. The deeper end of the ramp had an Ra of 29nm. Debris in the form of particles of diameter 200 - 700nm was apparent and would necessitate the use of a Flow Cell or similar debris extraction system in order to minimize. Total ablation depth at the deep end was 96µm, and the ramp had a length of 1665µm.

## **5. CONCLUSION**

Excimer laser ablation may be used to produce 2.5D or 3D structures in planar or non-planar materials. Careful consideration of fluence, optical NA and workpiece motion with co-ordinated CNC laser firing are all important in designing a practical laser machining tool. The recent availability of such machines has allowed the development of many different approaches to laser machining including mask projection, mask dragging, scanning masks, half-tone masks and programmed beam overlap.

Organic polymers are the most versatile and efficient materials to ablate by excimer laser by virtue of the photochemical interaction. Other materials can be machined, and further development of assist gases and vapours may increase the efficiency and hence reduce the cost of processing materials such as copper, steel silicon and others. For organic polymers structures may be machined to depths of the order of 800 to 1000µm with spatial resolutions of the order of 1µm. The control of ablated wall angle is closely linked to the fluence and optical NA used, but may also be controlled by appropriate choice of mask and processing method.

As the tools for excimer laser processing become more widely available, and particularly as the software required to turn a CNC system into a CAM system is developed, we expect to see an increased use of excimer laser micromachining as a complimentary tool to chemical etching, ion-beam milling and photolithography enabling the microengineer to design using a greater range of materials and shapes.

## **6. ACKNOWLEDGMENTS**

The authors would like to acknowledge the kind assistance of Don Purdey in the preparation of the halftone mask, and Mike Scott for performing the ablation experiment and producing the SEM images. Adrian Simcox made the profile measurements on the ablated samples. The nickel structure in figure 15 is shown by kind permission of Gilbert Morsch of Robert Bosch Laboratories.

## **7. REFERENCES**

1. P T Rumsby and M C Gower. "Excimer laser projector for microelectronics applications" SPIE Vol. 1598 Lasers in Microelectronic Manufacturing pp 98-108,(1991)
2. M D Levenson "Wavefront engineering for photolithography", Physics Today, 28 - 36, (1993)

3. N H Rizvi, M C Gower, F C Goodall, G Arthur and P Herman. "Excimer laser writing of submicrometer period fibre Bragg gratings using phase-shifting mask projection". *Electronics Letters* Vol 31 No. 11 pp 901-902 (1995)
4. J Arnold, U Dasbach, W Ehrfeld, K Hesch and H Lowe. "Combination of Excimer Laser Micromachining and Replication Processes Suited for Large Scale Production. *Applied Surface Science* 86 pp 251-258 (1995)
5. K. Zimmer. *Private Communication*, Institut für Oberflächenmodifizierung e.V., Leipzig, Germany 6.H K Tonshoff, D Hesse, H Kappel and J Mommsen, Laser Zentrum Hannover, "Excimer Laser Systems" *Laser Assisted Net shape Engineering, Proc. of the LANE'94 Vol 11* ed M Geiger and F Vollertsen, pp 627-650 (1994)
7. D W Thomas, C Foulkes-Williams, P T Rumsby and M C Gower. "Surface modification of polymers and ceramics induced by excimer laser radiation". *Laser Ablation of Electronic Materials*, ed E Fogarassy and S Lazare, Elsevier Science Publications, pp 221-228 (1992)

**This Page is Inserted by IFW Indexing and Scanning  
Operations and is not part of the Official Record**

**BEST AVAILABLE IMAGES**

Defective images within this document are accurate representations of the original documents submitted by the applicant.

Defects in the images include but are not limited to the items checked:

- ☒ **BLACK BORDERS**
- ☐ **IMAGE CUT OFF AT TOP, BOTTOM OR SIDES**
- ☐ **FADED TEXT OR DRAWING**
- ☐ **BLURRED OR ILLEGIBLE TEXT OR DRAWING**
- ☐ **SKEWED/SLANTED IMAGES**
- ☐ **COLOR OR BLACK AND WHITE PHOTOGRAPHS**
- ☐ **GRAY SCALE DOCUMENTS**
- ☒ **LINES OR MARKS ON ORIGINAL DOCUMENT**
- ☐ **REFERENCE(S) OR EXHIBIT(S) SUBMITTED ARE POOR QUALITY**
- ☐ **OTHER:** \_\_\_\_\_

**IMAGES ARE BEST AVAILABLE COPY.**

**As rescanning these documents will not correct the image problems checked, please do not report these problems to the IFW Image Problem Mailbox.**